Title: Advanced Cuttings Transport Study

Type of Report: Quarterly Technical
Reporting Period Start Date: April 1, 2004
Reporting Period End Date: June 30, 2004

Principal Authors:
Stefan Miska, Principal Investigator
Nicholas Takach, Co-Principal Investigator
Kaveh Ashenayi, Co-Principal Investigator
Ramadan Ahmed, Research Associate
Mengjiao Yu, Research Associate
Mark Pickell, Project Engineer
Len Volk, Research Associate
Mike Volk, Project Manager
Lei Zhou
Zhu Chen
Sameer Nene
Jagruthi Godugu

Date of Issue: July 31, 2004
DOE Award Number: DE-FG26-99BC15178

The University of Tulsa
600 South College Avenue
Tulsa, Oklahoma 74104

DISCLAIMER

ABSTRACT

We have tested the loop elevation system. We raised the mast to approximately 25 to 30 degrees from horizontal. All went well. However, while lowering the mast, it moved laterally a couple of degrees. Upon visual inspection, severe spalling of the concrete on the face of the support pillar, and deformation of the steel support structure was observed. At this time, the facility is ready for testing in the horizontal position. A new air compressor has been received and set in place for the ACTS test loop. A new laboratory has been built near the ACTS test loop

Roughened cups and rotors for the viscometer (RS300) were obtained. Rheologies of aqueous foams were measured using three different cup-rotor assemblies that have different surface roughness. The relationship between surface roughness and foam rheology was investigated.

Re-calibration of nuclear densitometers has been finished. The re-calibration was also performed with 1% surfactant foam. A new cuttings injection system was installed at the bottom of the injection tower. It replaced the previous injection auger.

A mechanistic model for cuttings transport with aerated mud has been developed. Cuttings transport mechanisms with aerated water at various conditions were experimentally investigated. A total of 39 tests were performed. Comparisons between the model predictions and experimental measurements show a satisfactory agreement.

Results from the ultrasonic monitoring system indicated that we could distinguish between different sand levels. We also have devised ways to achieve consistency of performance by securing the sensors in the caps in exactly the same manner as long as the sensors are not removed from the caps. A preliminary test was conducted on the main flow loop at 100 gpm flow rate and 20 lb/min cuttings injection rate. The measured bed thickness using the ultrasonic method showed a satisfactory agreement with nuclear densitometer readings. Thirty different data points were collected after the test section was put into liquid holdup mode. Readings indicated 2.5 to 2.7 inches of sand. The corresponding nuclear densitometers readings were between 2.5 and 3.1 inches.

Lab tests were conducted to check an on-line viewing system. Sharp images were obtained through a CCD camera with the use of a ring light or fiber light. A prototype device for measuring the average bubble size for the foam generator-viscometer was constructed from a ½" fitting. The new windowed cell has been received and installed on the ACTF Bubble Characterization Cart.

TABLE OF CONTENTS

LIST OF TABLES

LIST OF FIGURES

1. EXECUTIVE SUMMARY

Flow Loop Construction (Task 5)

On Wednesday June 23rd we raised the mast on the ACTS flow loop for the first time. The initial lift worked well. For the sake of safety we used a large fork lift in conjunction with the hydraulic cylinders. With the assist of the fork lift we raised the mast approximately 10 degrees. We then continued upward using only the hydraulic cylinders to approximately 25 to 30 degrees inclination. All went very well.

We decided next to lower the mast and lift from horizontal without the assist of the fork lift. While lowering the mast, it moved laterally a couple of degrees. Upon visual inspection, severe spalling of the concrete on the face of the support pillar, and deformation of the steel support structure was observed. With the aid of a crane, the mast was then lowered to its original horizontal position. At this time, the facility is ready for testing in the horizontal position. Elevation capabilities will be available again as soon as repairs are made.

A new air compressor has been received and set in place for the ACTS test loop. The cuttings injection system has been retro-fitted with a Moyno rotor and stator in order to improve the precision of cuttings injection.

A new laboratory has been built near the ACTS test loop It is located immediately behind the existing Control Building to serve on-going test loop experiments with auxiliary laboratory equipments such as the Fann 75 viscometer, the Foam Generator/Viscometer, and the DTF flow loop. The proximity to the existing ACTS flow loop will provide important support to the work being done there.

Additional items completed this quarter include:

- Install drill pipe in the annular section on the mast;
- Assemble drill pipe rotation system on the mast;
- Calibrate cuttings injection system;
- Calibrate injection tower weight measurements and install flexible hoses;
- Calibrate removal tower weight measurements and install flexible hoses;
- Complete stainless lines for vent and DP transmitters;
- Install inclinometer and wiring;
- Install nuclear densitometers and wiring;
- Calibrate nuclear densitometers;
- Calibrate hardware;

Foam Rheology Measurement and Development of a Foam Generator/Viscometer for EPET Conditions (Task 9b)

As mentioned in the preceding report, machining of the cups and rotors took approximately a year and a half; and it was not possible to perform foam rheology tests with roughened cups and rotors. As a result, a contract with a new machine shop was signed and roughened cups and rotors were made. Foam rheology tests were conducted using smooth and roughened cup-rotor assemblies. The Foam Generator/Viscometer was used to generate different quality foams. Surfactant (Weatherford KLEAN-FOAM™) concentrations

in the liquid phase for all the tests were 1 percent by volume. Rheologies of foams were measured using three different cup-rotor assemblies that have different surface roughness. The relationship between surface roughness and foam rheology was investigated.

Study of Cuttings Transport with Foam under Elevated Pressure and Elevated Temperature Conditions (Task 13)

Task 13 is a continuation of two other research tasks (Task #6 and Task #9) on foam rheology and cuttings transport. Literature survey, mathematical modeling, and preliminary rheology and cuttings transport tests are well advanced. This task will extend beyond the 5-year DOE project timeline. It is scheduled to be completed in August, 2005.

The objectives of this project are: i) to investigate experimentally foam rheology under EPET conditions using pipe viscometers; ii) to determine experimentally volumetric requirements for effective cuttings transport with foam in horizontal wellbores without pipe rotation; iii) to develop a mechanistic cuttings-transport model; and iv) to verify the cuttings transport predictions of the model with experimental data.

Re-calibration work for two nuclear densitometers has been finished. A multiphase cuttings injection system (Moyno progressive cavity pump) was installed at the bottom of the injection tower. It replaced the previous injection auger.

Study of Cuttings Transport with Aerated Mud Under Elevated Pressure and Temperature Conditions (Task 10)

A mechanistic model for cuttings transport with aerated mud has been developed. The hydraulics of one-dimensional, two-phase (gas-liquid) flow is coupled with the mechanisms of cuttings transport in the formulation of the model. The model determines the flow pattern and predicts the in-situ cuttings concentration, mixture density and frictional pressure losses in a horizontal concentric annulus. Details of the mechanistic model were described in the last DOE quarterly report. The influences of gas-liquid ratio and other flow parameters on the bottom-hole pressure, frictional pressure loss and cuttings transport are analyzed using these model.

Cuttings transport mechanisms with aerated water at various conditions (different air and water flow rates, different pressures and temperatures) were experimentally investigated. A total of 39 tests were performed. Comparisons between the model predictions and experimental measurements show satisfactory agreement.

Research on Instrumentation to Measure Cuttings Concentration and Distribution in a Flowing Slurry (Task 11)

Since the printed circuit board is functioning with acceptable noise level we were able to conduct several tests. We used the newly designed pipe test section & The DFT test facility to conduct tests.

The results indicated that we could distinguish between different sand levels. We also have devised ways to achieve consistency of performance by securing the sensors in the caps in exactly the same manner as long as the sensors are not removed from the caps. It should be noted that the caps could be removed from the pipe for adding sand. We tested with water, air and a mix of the two mediums.

The data acquisition software development is continuing. The preliminary results indicate that we are able to distinguish between different sand concentrations. We have further modified the software and the firmware to improve the accuracy.

To account for the nonlinear nature of the fluid flow we are using a neural network method to analyze the data being collected. We have purchased a commercial neural network development package. We have developed a large number of neural network based analysis models.

A preliminary test was conducted on the main flow loop at 100 gpm flow rate and 20 lb/min cuttings injection rate. The measured bed thickness using the ultrasonic method showed a satisfactory agreement with nuclear densitometer readings. Thirty different data points were collected after the test section was put into liquid holdup mode. Readings indicated 2.5 to 2.7 inches of sand. The corresponding nuclear densitometers readings were between 2.5 and 3.1 inch.

Development of Foam Bubble Size and Distribution Monitoring System (Task 12)

Lab tests were conducted to check an on-line vision system. Sharp images were obtained through a CCD camera with the use of a ring light or fiber light. Preliminary results indicate that the fiber light provides a better image while the ring lights show reflection problems. During lab tests it was found that up to 15 frames per second can be achieved when grabbing continuous images. The “Client-Server” control system was tested in the lab. Tests results showed good response rate.

A prototype device for measuring the average bubble size for the foam generator-viscometer was constructed from a ½” fitting. Light is supplied by a white light-emitting diode at the top of the photo, and the transmitted light is recorded by a photodiode. Both the LED and photodiode are separated from the foam by small glass windows.

The new windowed cell has been received and installed on the ACTF Bubble Characterization Cart (“the Cart”). The cell is designed to: i) eliminate the dead volume that occurs in standard windowed flow-through cells; allow better illumination of flowing foam; and iii) maintain a nearly uniform cross-section to flow through the cell.

Safety Program for the ACTS Flow Loop (Task 1S)

Safety issues are frequently discussed with the students. The importance of safety is well understood by the students and the staff involved in the project.

SUMMARY OF CURRENT TASKS FOR ACTS PROJECT

Table 1.1 Summary of ACTS Project Plan Execution

ID	Task Name	Status
Task 1	Construction of Elevated Temperature Facility	Completed
Task 2	Construction of Aeration System	Completed
Task 3	Construction of Cuttings Injection/Separation Facility	Completed
Task 4	Construction of Drill Pipe Rotating Facility	Completed
Task 5	Construction of Loop Inclination Facility	Completed+
Task 6	Research on Cuttings Transport with Foam at LPAT Conditions	Completed
Task 7	Research on Cuttings Transport with Aerated Mud at LPAT conditions	Completed
Task 8	Research on Synthetic Drilling Fluids at EPET Conditions	Completed
Task 9	Research on Foam flow under EPET Conditions	Completed
Task 9b	Development of a Foam Generator/Viscometer for EPET Conditions	Completed
Task 10	Research on Cuttings Transport with Aerated Mud at EPET conditions	Completed
Task 11	Development of Cuttings Monitoring System	Completed++
Task 12	Development of Foam Bubble Size and Distribution Monitoring System	Completed
Task 13	Research on Cuttings Transport with Foam at EPET Conditions	40%
Task S1	Development of a Safety Program	continual

+ Requires modifications of mast support structure
++ Requires additional training of the Neural Network System

It should be noted that all the 12 original Tasks of the 5-year program have been completed. The percentage of completeness refers to the plan proposed in the original proposal.

As we begin the steady state phase of the project, our plan is to carry on the research activities and continue improvements in the flow loop components. Future activities will be consulted with our industry partners.

2. ACTF DESIGN AND CONSTRUCTION ACCOMPLISHMENTS (TASK 5)

2.1 ACTF Design and Construction Accomplishments

The major construction activities for this quarter are: i) installation of hydraulic cylinders; ii) reinstallation of test section and drill pipe rotation system on the mast; iii) installation of a new cuttings injection system; and iv) installation of flexible hoses at the inlets and outlets of the injection and separation towers.

After installation of the mast, the annular test section and pipe rotation system were reassembled. One additional view port was installed in the test section. Nuclear densitometers have been calibrated and reinstalled. During the installation, the densitometers have been reoriented to fit with the test section and its support system. The expansion tank was relocated to beneath the mast support (Fig. 2.1).

Fig. 2.1 Mast together with the hydraulic cylinders

We received the hydraulic cylinders from the manufacture after re-work of the clevis ends, which were so closely spaced together as to restrict the rotation of the mast. The cylinders were carefully assembled to meet all in the original design and installation specifications. As shown in Fig. 2.1, one end of each cylinder is welded to a steel I-beam sub-structure, which is imbedded in the concrete base.

On Wednesday June 23rd, 2004, we raised the mast on the ACTS flow loop for the first time. The initial lift worked well. As a precaution we used a large fork lift in conjunction with the hydraulic cylinders. With the assist of the fork lift we raised the mast approximately 10

degrees (Fig. 2.2). We then continued upward using only the hydraulic cylinders to approximately 25 to 30 degrees inclination (Figs. 2.3a & 2.3b). All went very well.

Fig. 2.2 Mast when raised approximately 10 degrees

(a)

(b)

Fig. 2.3 Mast section at approximately 25 to 30 degree inclination

We decided next to lower the mast and lift from horizontal without the assist of the fork lift. While lowering the mast, it moved laterally a couple of degrees. Upon visual inspection, severe spalling of the concrete on the face of the support pillar, and deformation of the steel support structure, was observed. With the aid of a crane, the mast was then lowered to its original horizontal position.

No damage appears to have occurred in the mast itself, the hydraulic cylinders, attachment points for the hydraulic cylinders, the concrete base, the steel I-beam sub-structure, the attachment j-bolts, or the concrete pillar other than superficial spalling on two corners. The support structure is sound and will continue to provide excellent support to the mast for all future experiments in the horizontal configuration. The support structure will, however, have to be re-built to be able to operate the mast in any elevated configuration.

There is not one single component or action that stands out as the definitive explanation of failure of the support structure. Certainly in the higher stress condition created during the initial lift of the mast from horizontal, and through continued lifting, no problems were evidenced at all. Quite the contrary, knowing we were past the critical stress stage it was a moment of congratulation that all was going flawlessly. When the mast was begun to be lowered, however, one cylinder obviously favored the other and torsion was imposed to such a degree that the support structure became deformed (see Fig. 2.4). The design of the support structure is shown in Fig. 2.5.

Fig. 2.4 Deformed mast support structure

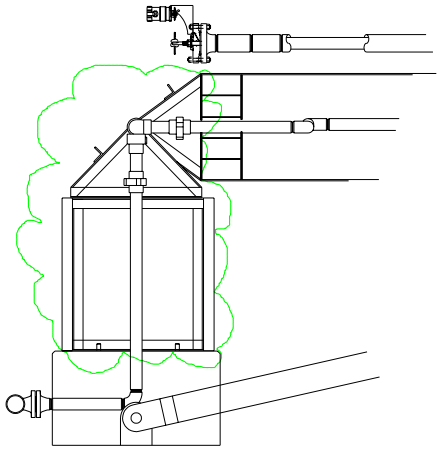

Fig. 2.5 Design of mast support

As it became deformed, the front corners (those corners closest to the hydraulic cylinders and resting on the concrete) imposed a point load onto the concrete and caused it to spall off in those areas. As the mast was continued to be lowered, the support structure further deformed, and the mast rotated.

The mechanism which caused one cylinder to be favored is complex beyond our means to understand at this juncture. Perhaps when we are able to disassemble the support structure we will learn more. Without any instrumentation on the cylinders to monitor the pressure on each cylinder's piston we can't say absolutely that, for example, one cylinder received more pressure than the other and that caused the torsion. We do know how the hydraulic pump and the valves and lines that go to the cylinders work and we can see that it should not be possible for one cylinder to see more pressure than the other.

It is reasonable to assume that the hydraulic cylinders are not perfectly matched and therefore, even when pressurized the same amount, there would be some minor differences in their resulting force. But this should be negligible and no difference was apparent when the mast was being raised. Also, it is reasonable to assume that the cylinders were not

installed with sufficient precision as to be perfectly complimentary to each other and not have any tendency whatsoever to want to push the mast either left or right but this too should be negligible and no difference was apparent when the mast was being raised.

The same could be said for friction in the pivot pin, alignment of the pivot pin to the axis of rotation, friction in the clevis ends of the cylinders and the alignment of those ends.

However, due to the length of the mast there is an opportunity to magnify any tendencies toward misalignment. Also, there was no overt effort to design the support structure for strength against torsion. Therefore, it is our hypothesis that the hydraulic cylinders not pushing at the same rate was the primary causative problem. Repairs, of course, are dependant on the availability of sufficient budget; however we anticipate that the repairs we will proceed with will include a support structure which will be resistant to torsion and a means by which the cylinders may be collectively monitored and individually controlled. We will be consulting with others who have experience with hydraulic systems similar to this to help us.

At this time, the facility is ready for testing in the horizontal position. As reported in last quarter's report, a new air compressor has been purchased for the ACTS test loop. Pictured below (Fig. 2.6), this compressor has been and set in place.

Fig. 2.6 New air compressor

A new air flow meter and control valve have been purchased and are being installed as indicated in Fig. 2.7.

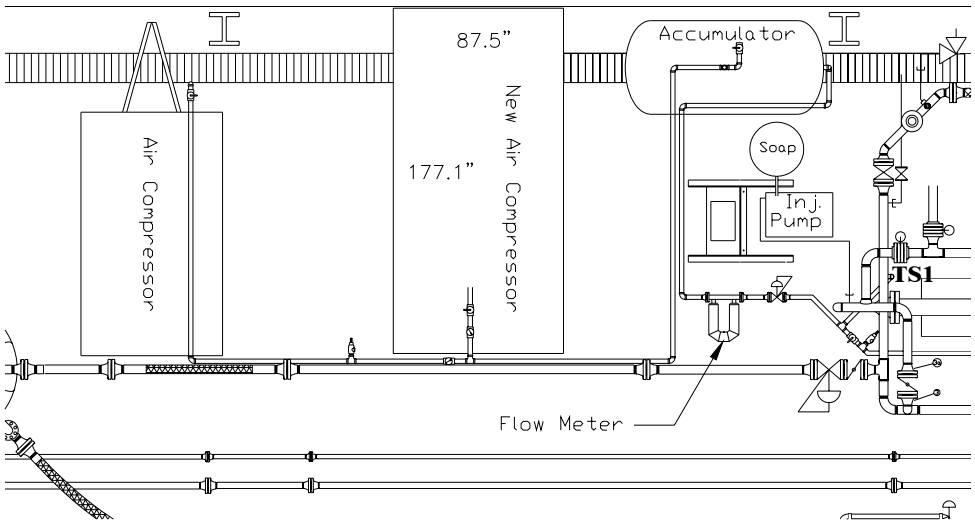

Fig. 2.7 New air flow meter

The cuttings injection system has been retro-fitted with a Moyno rotor/stator in order to improve the precision of cuttings injection. The original design consisted of a screw auger (Fig. 2.8) located vertically beneath the injection tower (Fig. 2.9).

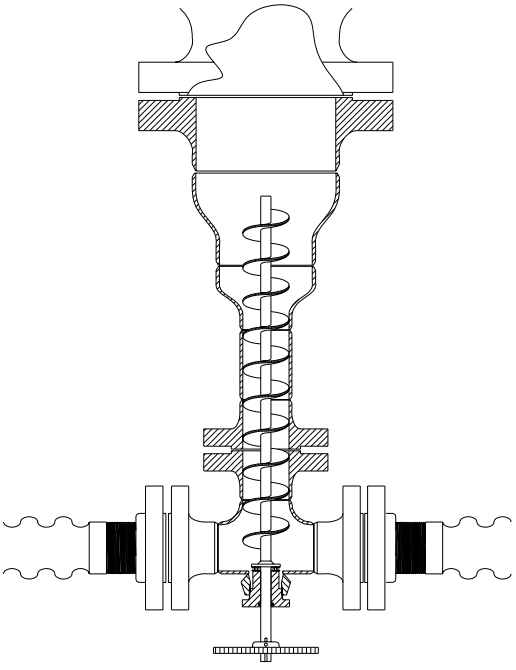

Fig. 2.8 Screw auger

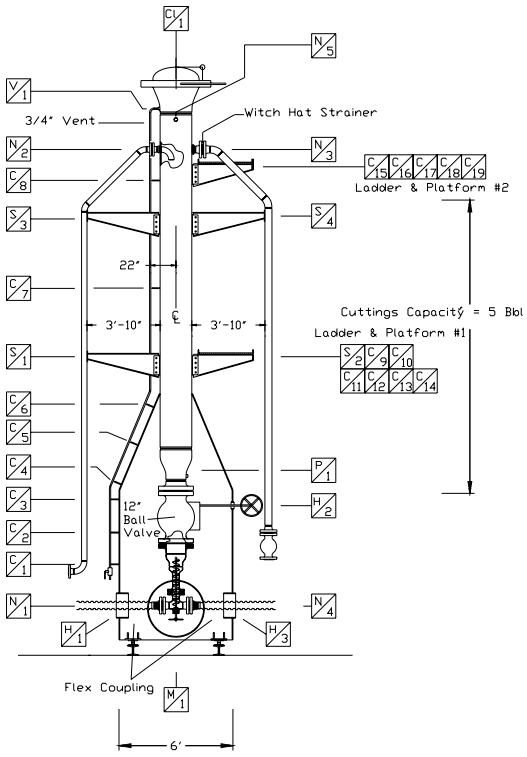

Fig. 2.9 Injection tower

This system proved to work adequately but room was left for improvement. The screw auger was shown to self-feed under certain circumstances. Therefore, a rotor/stator design (Fig.

2.10) such as that used by Moyno is expected to give superior results without any tendency to self-feed.

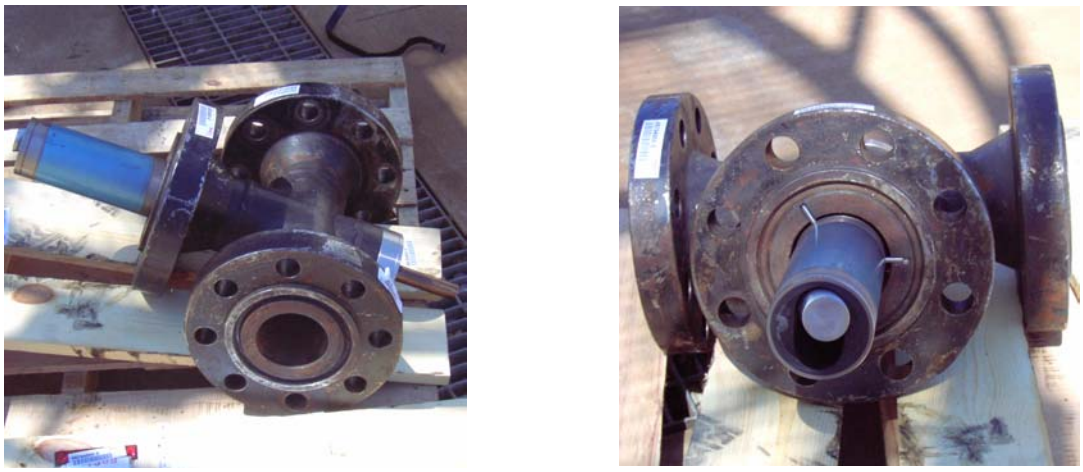

Fig. 2.10 Cuttings injection system (Moyno rotor/stator design)

A new laboratory has been built near the ACTS test loop. The floor plan of the laboratory is presented in Fig. 2.11. It is located immediately behind the existing Control Building to serve on-going test loop experiments with auxiliary laboratory equipments such as a Fann 75 viscometer, the Foam Generator/Viscometer, and the DTF flow loop. The proximity to the existing ACTS flow loop will provide important support to the work being done there. Figures 2.12 and 2.13 show pictures of the lab.

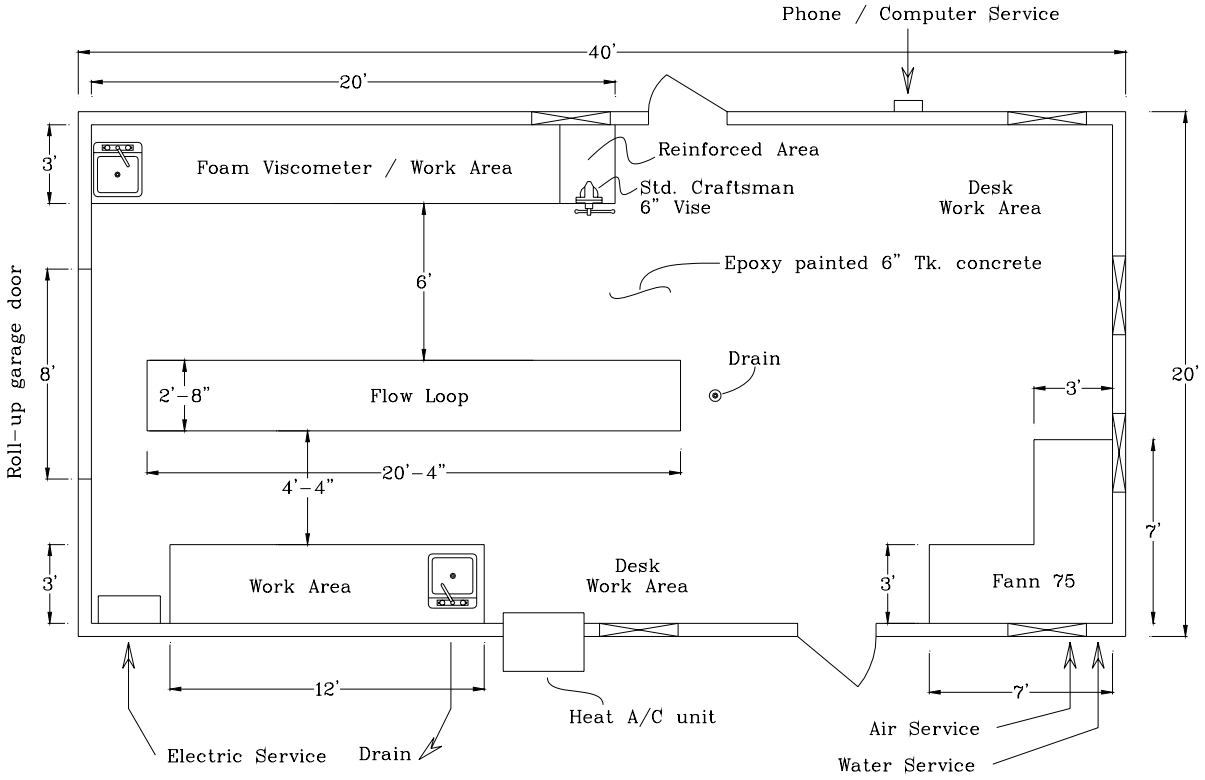

Fig. 2.11 Floor plan of new laboratory

Fig. 2.12 New laboratory (outside)

Fig. 2.13 New laboratory (inside)

Additional items completed this quarter include:

- Calibration of cuttings injection system;
- Calibration of injection tower weight measurements and installation of flexible hoses;
- Calibration of removal tower weight measurements and installation of flexible hoses;
- Installation of stainless lines for vent and DP transmitters;
- Installation of inclinometer and wiring;
- Calibration of hardware;

3. STUDY OF FOAM RHEOLOGY USING ROTATIONAL VISCOMETER AND DEVELOPMENT OF FOAM VISCOMETER/GENERATOR (TASK 9B)

Abstract

A major factor that must be considered when measuring the rheology of foam is the phenomenon of "wall slip." In order to quantify this phenomenon, a variety of roughnesses must be applied to the surfaces that the foam is in contact with while rheology measurements are being made.

As mentioned in the last report, the machining of the cups and rotors took approximately a year and a half. As a result it was not possible to perform foam rheology tests with roughed cups and rotors. A contract with a new machine shop was signed and roughened cups and rotors were made. Foam rheology tests were conducted using a smooth cup-rotor assembly and for the first time, experiments were conducted with roughened cup-rotor assemblies. The Foam Generator/Viscometer was used to generate different quality foams. Surfactant (Weatherford KLEAN-FOAM™) concentrations in the liquid phase for all the tests were 1 percent by volume. Rheologies of foams were measured using three different cup-rotor assemblies that have different surface roughness. The relationship between surface roughness and foam rheology was investigated.

3.1 Introduction

To measure foam rheology, one commonly-used method is by using a pipe viscometer; normally three pipes are required to determine if there is "wall slip". A pipe viscometer such as a large-scale flow loop can be expensive to operate. Three hurdles need to be overcome to use a rotational viscometer to measure foam rheology. First, to develop a new instrument that will enable the generation of foams with controllable foam properties (such as bubble size); second, to develop a process that will enable measurements of the viscous properties of foams that are free of the influences of drainage and bubble coalescence; and third to be able quantify the effects of surface roughness on wall slip. This led to the development of a new foam generator and viscometer.

A new foam generator/viscometer that is developed in ACTS project is currently operational. This instrument is capable of controlling the following six variables independently. i) Foam quality, ii) pressure, iii) temperature, iv) surfactants and other additives; v) bubble size, and vi) surface roughness inside the viscometer (Thermo Haake RS 300).

The Foam Generator/Viscometer provides a means by which the rheology of foams may be measured. Surfactant and water are combined with air in various ratios, foam is generated in the foam generator and allowed to flow under controlled conditions (pressure, temperature, and flow rate) through a modified (variable surface roughness) Couette-type rotational viscometer at such a rate that the viscosity of the foam is determined while its properties (bubble size, quality, pressure, temperature) are held constant.

3.2 Description of the Foam Generator/Viscometer

Figures 3.1 and 3.2 show a schematic and picture of the Foam Generator/Viscometer, respectively. Some important features of this Foam Generator/Viscometer are: i) a cylinder (Fig. 3.3) with a movable dome-shaped piston inside, which separates the cylinder into two chambers (mixing chamber and pneumatic chamber) and that assists recirculation of the fluids back down along the sidewalls of the chamber; ii) a caliper installed to measure the rate of movement of the piston, iii) a propeller that can be changed to permit the use of variety of designs, iv) a variable speed drive motor than turn the propeller over a wide range of rotary speeds, v) view ports to enable visual observations of the foam and/or perform optical measurements of foam properties such as bubble size.

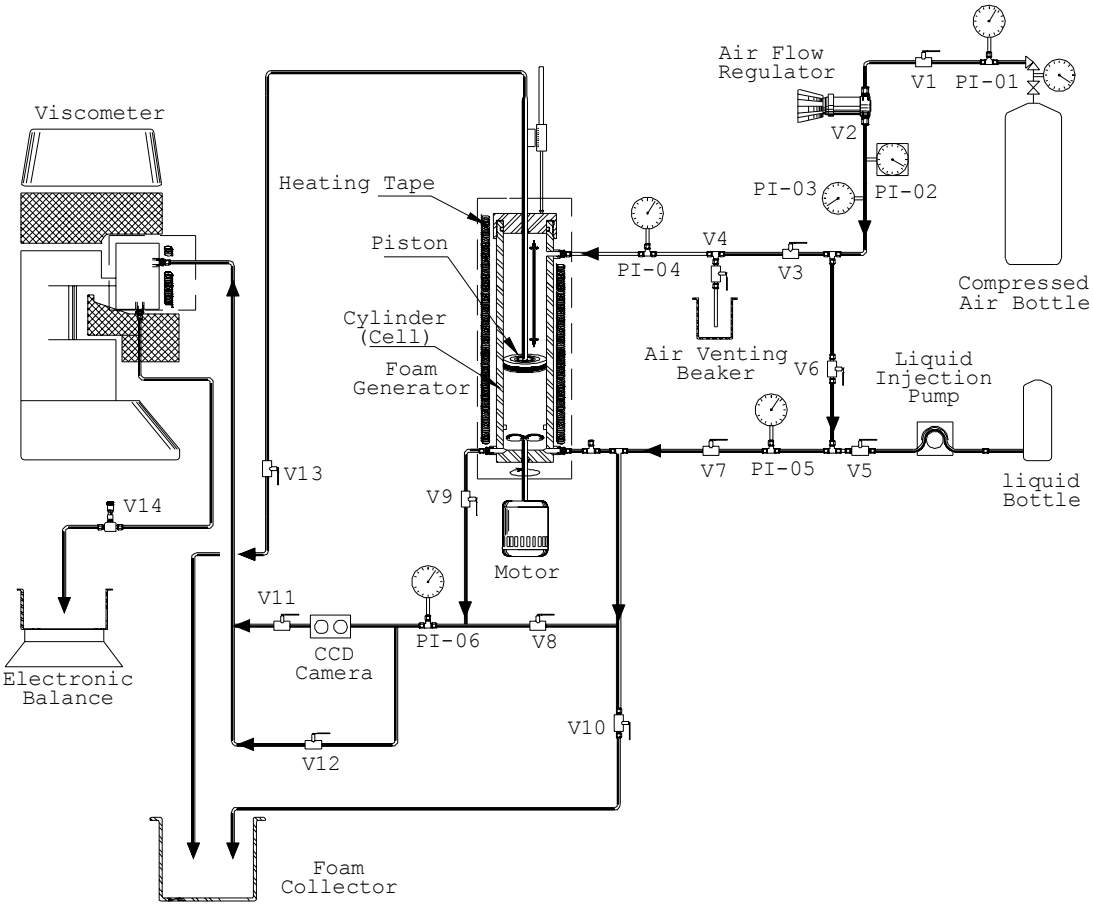

Fig. 3.1 Schematics of the Foam Generator/ Viscometer

Some auxiliary components are necessary for proper functioning of the Foam Generator/Viscometer; these are: i) a low-volume metering pump (Fig. 3.4) that can meter and pump proper the amount of liquid into the mixing chamber; and ii) a gas source (Fig. 3.4) with pressure regulators, gauges and control valves to introduce gas at a selected pressure into the mixing chamber and the pneumatic chamber. The pneumatic chamber maintains constant pressure in the mixing chamber when foam flows from the mixing chamber to the viscometer.

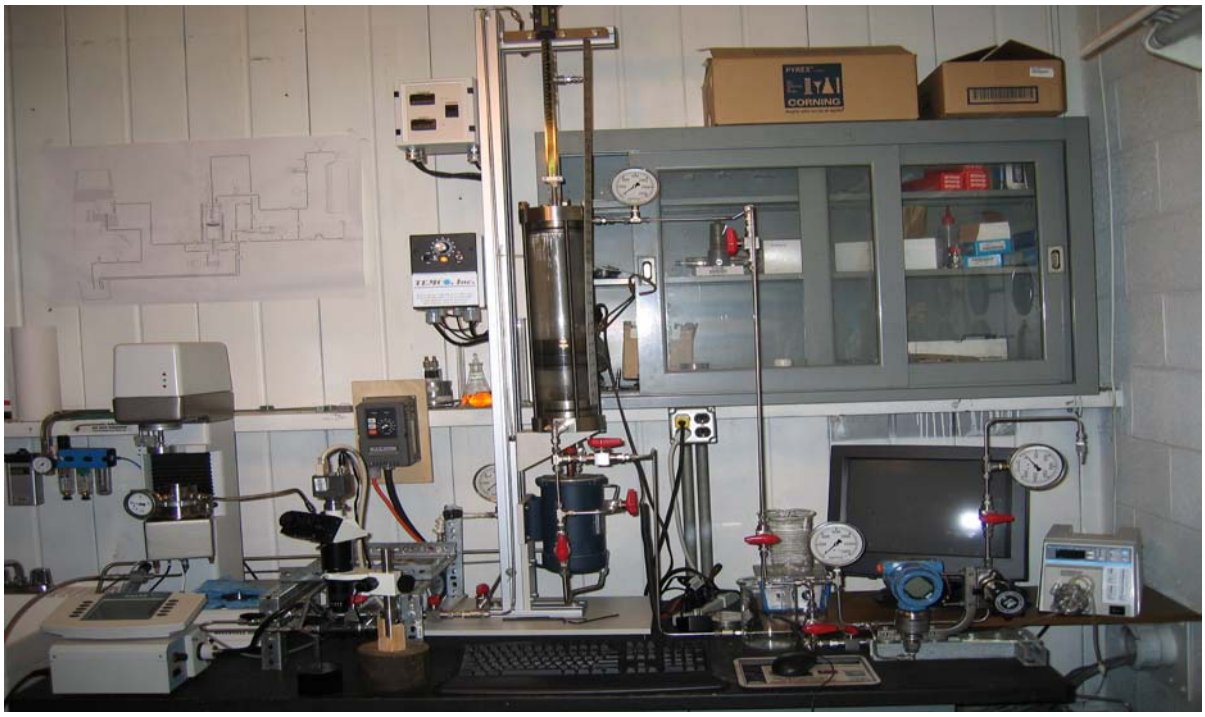

Fig. 3.2 Foam Generator/ Viscometer

Fig. 3.3 Foam generator cylinder

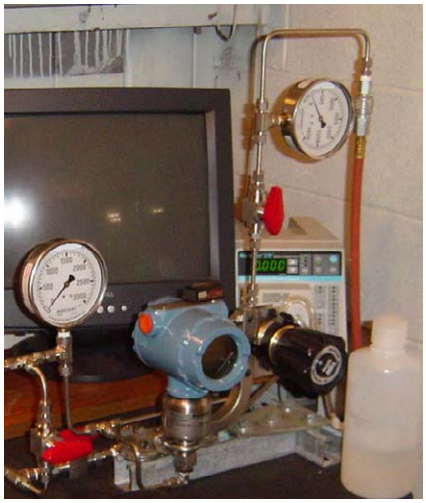

Fig. 3.4 Air and liquid injection systems

The Thermo Haake RS 300 viscometer (Fig. 3.5) was specifically selected because it enables foam to enter at the top of the measurement cup and leave at the bottom; thus, during the rheology measurement process, any foam degradation such as drainage and bubble coalescence is compensated by introducing new foam into the measuring cup. It allows using rotors with different roughnesses; and rotary speeds to give a controlled shear rate. It also has elevated pressure and temperature measurement capabilities. The foam texture can be assessed at the view-port upstream of the viscometer using a microscope and CCD camera (Fig. 3.6).

Fig. 3.5 Viscometer (RS300)

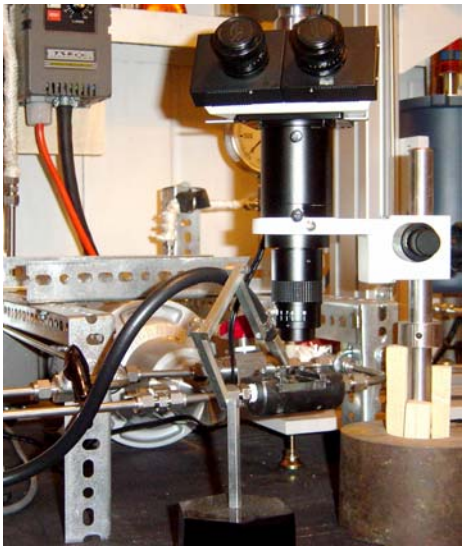

Fig. 3.6 Microscope and CCD Camera

An essential feature of this Foam Generator/Viscometer is that once a constant-property foam is generated, valves are manipulated to inject gas to the pneumatic chamber to maintain constant pressure on the foam. Foam flows from the generator to the viscometer when a micrometer valve (V14) downstream of the viscometer is opened. The rate at which the foam flows out of the generator is determined by measuring liquid phase mass flow rate at the outlet of the viscometer with an electronic balance. In order to carry out a foam experiment, some basic calculations need to be performed. Table 3.1 shows design parameters of the foam generator.

Table 3.1 Design Features of Foam Generator

Symbols	Descriptions	Value
D_P	Piston diameter	4.5”
V_C	Chamber volume per height	100 ml /0.43”
V_T	Tubing volume between the liquid pump and mixing chamber	34 ml
V_M	Volume of metal in the tapered edge of the mixing chamber	29.5 ml
V_G	Volume left in the lower part (grove) of the mixing chamber after drainage	11.1 ml
V_D	Volume of the depression in the lower side of piston	50 ml
V_{SP}	Volume of the shaft and propeller	27.5 ml

During the experiments, the liquid phase volume for a given quality foam is calculated as:

$$V_L = (1-\Gamma)(D_P V_C - V_{SP} - V_M + V_D + V_G) \tag{3.1}$$

The process of foam generation requires flushing of the injection lines and the mixing chamber with surfactant solution for cleaning purposes. After flushing, there is 11.1 ml of surfactant solution left in the chamber. Therefore, the amount of liquid injected is:

$$V_{inj} = V_L - V_G \tag{3.2}$$

3.3 Test Procedure

Rheology tests consisted of foam generation, and rheology and bubble size measurements. Tests were performed at different foam qualities and cup-rotor assemblies. The test procedure includes the following steps:

1. Pump a measured volume of surfactant solution into the mixing cell;
2. Fill the cell with gas at a given pressure;
3. Charge the flow line between the generator and viscometer with the same gas pressure;
4. Turn on propeller and let it run until the foam equilibrates (by physical observation);
5. Vent equilibrated foam via the viscometer while maintaining constant pressure by applying gas pressure on the pneumatic chamber. In this way, foam quality is kept constant during the test;
6. When homogenous foam flows out of the viscometer, measure the liquid phase mass flow rate using the electronic balance and stop watch, and adjust the micrometer needle valve to keep the mass flow rate in the optimum range. Figure 3.7 presents optimum liquid phase flow rate required to maintain foam flow rate of 15 ml/min;
7. Measure the foam rheology;
8. Stop the propeller, and take a picture of the foam in the view port with the CCD camera and microscope;
9. Stop test.

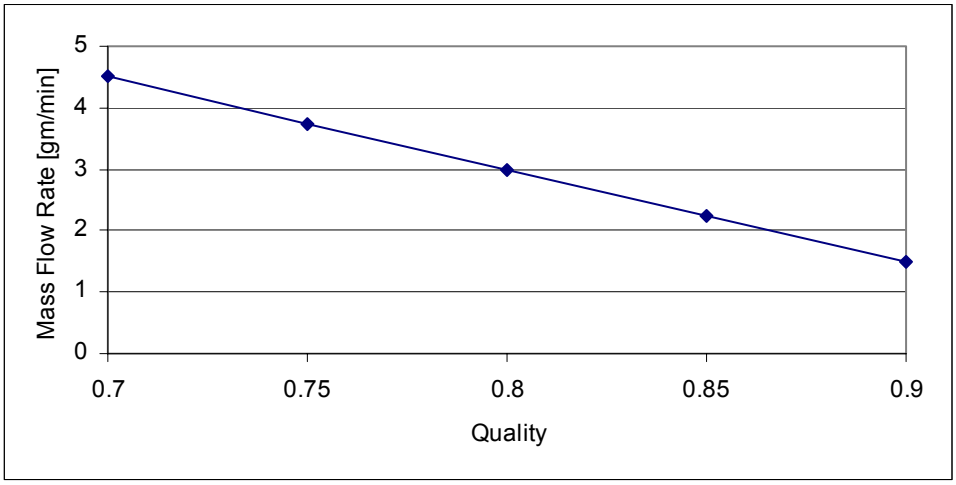

Fig. 3.7 Optimum liquid phase mass flow rate vs. foam quality

3.4 Test Matrix

The test matrix is shown in Table 3.2. According to this test matrix, type of foam formulation, pressure, and temperature were fixed. The wall roughnesses of three cup-rotor assemblies were varied in order to quantify the effect of wall slip on rheology measurements. Concentration of surfactant (Weatherford KLEAN-FOAM™) was 1% by volume in all the experiments. Test temperature and pressure were controlled at 25°C and 25 psi. Five foam qualities were tested: 70%, 75%, 80%, 85%, 90%. All foams were generated using the foam

generator with the almost identical mixing times. The mixing time was sufficient to obtain stable and well-equilibrated foam.

Table 3.2 Test Matrix for Foam Generator/Viscometer Tests

	Test #1	Test #2	Test #3
Foam Formulation	1% Weatherford surfactant (KLEAN-FOAM™) by volume		
Quality	70%, 75%, 80%, 85%, 90%	70%, 75%, 80%, 85%, 90%	70%, 75%, 80%, 85%, 90%
T (°C)	25	25	25
P (psi)	25	25	25
Wall Roughness	Smooth	Roughness #1	Roughness #2

Another important issue during the test was how to maintain optimum foam flow rate through the viscometer. On one hand, it is important to allow enough foam to flow through the viscometer to eliminate the effect of foam drainage on the measurements; on the other hand, flow rate can not be so fast as to minimize axial shearing of the foam inside the viscometer. The optimum foam volume flow rate (approximately 15 ml/min) was obtained and controlled for each foam quality, based on the criteria of nominal axial shear rate less than 3 s^{-1} at the wall and an average foam residence time of 4 min in the viscometer. Our previous aqueous foam drainage experiments indicated that the half lifes of the test foams under static conditions are in the range of 10 to 12 minutes. Electronic balance shown in Fig. 3.1 is used to determine mass flow rate of foam passing through the viscometer. By controlling the micrometer valve (V14), the foam flow rate was maintained at the desired level.

The optimum foam volume flow rate is based on nominal Newtonian axial shear rate. Since the diameter of the rotor (36 mm) is 90% of the cup diameter (40 mm), the annulus between rotor and cup can be approximated with a narrow rectangular slot. Therefore, for a narrow slot, the axial flow shear rate is calculated as:

$$\gamma = \frac{12V}{D_o - D_i} = \frac{12 \times 1.05 \times 10^{-3}(m/s)}{4 \times 10^{-3}(m/s)} = 3(s^{-1}) \tag{3.3}$$

where axial flow velocity at 15 ml/min is calculated as:

$$V = \frac{Q}{A} = \frac{15 \times 10^{-6}(m^3/\min)}{2.387 \times 10^{-4}(m^3)} = 0.0628(m/\min) = 1.05 \times 10^{-3}(m/s) \tag{3.4}$$

Flow area, A is calculated as:

$$A = \frac{\pi}{4}(D_o^{\,2} - D_i^{\,2}) = 2.387 \times 10^{-4}(m^3) \tag{3.5}$$

For a Power Law fluid, axial flow shear rate at the wall is given by:

$$\gamma = \frac{1+2n}{3n}\frac{12V}{D_o - D_i} \tag{3.6}$$

According to Eq. 3.6, for a shear thinning case, the axial shear rate is a little higher than 3 s^{-1}, depending on the flow behavior index, n. For instance, for n = 0.5, the shear rate becomes 4 s^{-1}. For helical flow in a narrow annulus, the overall shear rate, γ_h, is approximately given by:

$$\gamma_h \approx \left(\gamma_r^2 + \gamma_a^2\right)^{0.5} \tag{3.7}$$

where γ_r and γ_a are rotational and axial flow shear rates. In order to reduce the effect of axial flow on the overall shear rate, $(\gamma_r)^2$ should be greater than $(\gamma_a)^2$. The minimum nominal rotational shear rate for the experiment was 10 s^{-1}. This means that the above criterion is fulfilled. Therefore, the effect of axial flow is minimized even for low shear rate measurements, which are highly affected with the axial flow.

3.5 Calibration Test

The purpose of calibrating this viscometer using viscosity standards is to correct for end effects and bearing drag. The end effects have a tendency to increase measured torque due to shearing of the fluid between the space above and below the rotor inside the cup (Fig. 3.8). Viscometer readings are based on the measured torque acting on the rotor. In addition to the size and geometry of the rotor, properties of the test fluid, end effects, and bearing drag all affect torque measurements. The basic purpose of a calibration test is to quantify the magnitude of the end effects and bearing drag so that they can be subtracted in order to obtain the actual torque required to shear the fluid in the gap.

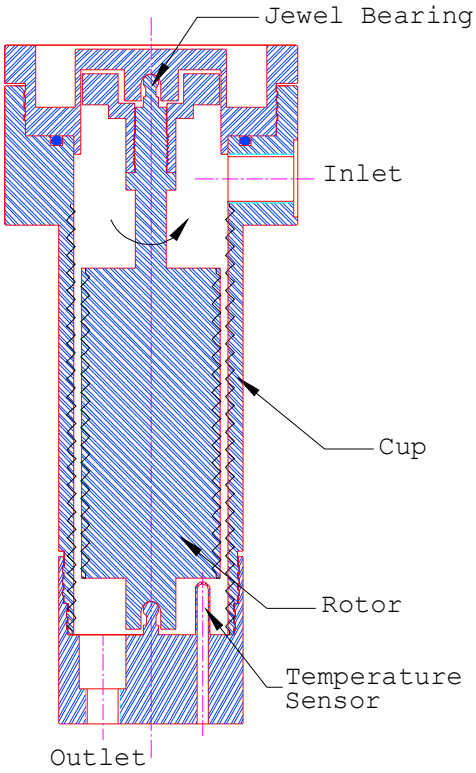

Fig. 3.8 Cup-rotor assembly of RS300

Four viscosity standards (calibration oils from Canon Instrument Company) with nominal viscosity 50 cP, 100 cP, 200 cP and 500 cP were used to calibrate the smooth cup-rotor assembly. This range of viscosity (i.e. 50 to 500 cP) covers most of the viscosity range of aqueous foams. Using the calibration oils, thirteen different viscosity data points (Table 3.3) were measured to calibrate the viscometer. Measured and calculated torques were compared. A calibration curve for each shear rate was prepared.

Table 3.3 Viscosity Standards Used for Calibrating the Viscometer

Nominal Viscosity (cP)	True Viscosity (cP)	Temperature (°C)
50	52.98	20.0
	43.31	30.0
	29.98	50.0
	21.58	70.0
100	105.4	20.0
	71.14	40.0
200	206.7	20.0
	170.32	29.6
	139.3	40.0
	116.7	50.0
	78.01	75.0
500	520.0	20.0
	349.5	40.0

The viscometer was calibrated at shear rates of 1000, 600, 400, 300, 200, 100, 50, 30, 20 and 10 s^{-1}. As expected, the measured torque is higher than the calculated torque for all the shear rates. The calibration curve, used for correcting the measured data at shear rate of 400 s^{-1}, is presented in Fig. 3.9. Similar curves are prepared to correct the measured torque at a given shear rate. After the calibration, corrected torques can be obtained from these curves. For foam tests, each measured torque corresponds to a corrected torque, and once the corrected torque is obtained, corrected shear stress can be obtained. A computer code was developed to interpolate between calibrated data points from the curve.

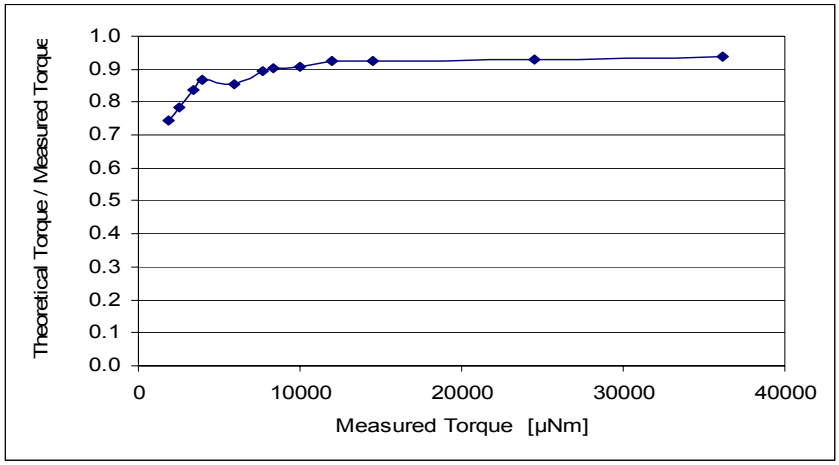

Fig. 3.9 Calibration curve obtained at 400 s-1 shear rate

Limited calibration tests were performed using the roughened cup-rotor assemblies to determine the effect of roughness and rotor weight on the calibration curve. One viscosity standard (200 cP nominal) was used for testing roughened cup-rotor assemblies at 20 and 40°C. Theoretically, without wall slip, the measurement should be the same for all the cup-rotor assemblies. Fig. 3.10 shows the measured torque using different cup-rotor assemblies as a function of shear rate using one viscosity standard at different temperatures. Approximately identical torque readings are recorded, which indicates that the cup-rotor assemblies are geometrically more or less identical and have the same friction drags. Therefore, any torque measurement difference resulting from different cup-rotor assembly is most probably due to other factors.

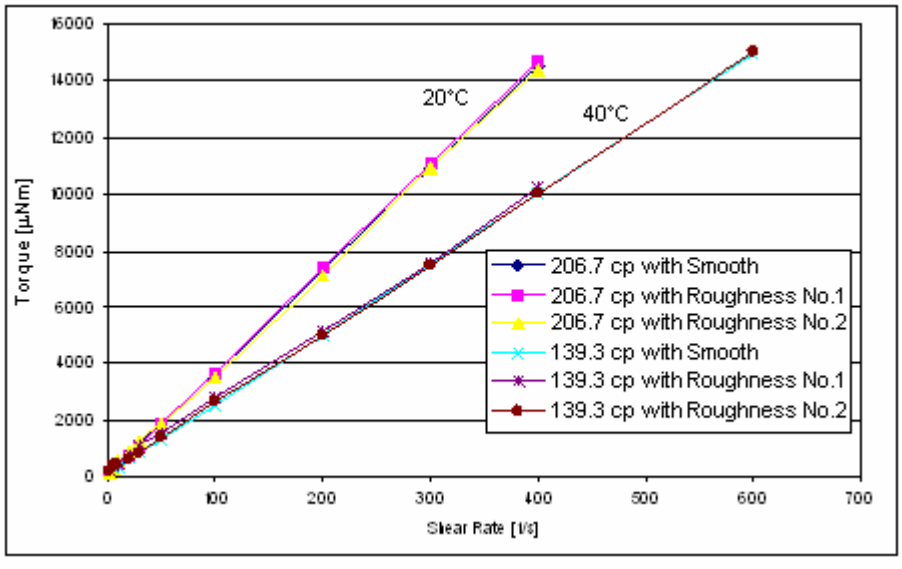

Fig. 3.10 Measured torques vs. shear rate for different cup-rotor assemblies

3.6 Quantification of Rough Surface

Quantification of rough surface required a roughness measuring instrument, which is commonly used by the surface coatings industry. Many possibilities were explored before purchasing of the roughness measuring instrument (Surftest 401). This instrument will provide an accurate surface roughness measurement, not only for rotors and cups, but also for the inside of the ACTS Flow Loop, in which hydraulic tests with foams are planned. The instrument has a diamond stylus that passes over the top of the roughened surfaces. This instrument is capable of evaluating surface textures including waviness with a variety of parameters according to various national and international standards. The measured results are displayed digitally and graphically on the touch panel, and output to a built-in printer. Some of the output includes: i) average roughness, Ra, which is the arithmetic mean of the absolute values of the profile deviations (Y_i) from the mean line; and ii) standard deviation of the surface roughness, Rq. The formulas for Ra and Rq are mathematically written as:

$$Ra = \frac{1}{N}\sum_{i=1}^{N} | Y_i | \qquad (3.8)$$

$$Rq = \left[\frac{1}{N} \sum_{i=1}^{N} Y_i^2 \right]^{0.5} \tag{3.9}$$

Two stainless steel cups with 0.025-inch and 0.010-inch surface roughnesses were manufactured. Rotors were also manufactured and milled to create diamond shaped projections from the surface to contain the slip layer and shear the foam. Surface roughness measurements were made twice. Initial measurements indicated that the 0.025-inch and 0.010-inch cups have average roughnesses of 10.31 μm and 14.85 μm respectively. The 0.025-inch and 0.010-inch describe the distance from one peak to the next peak of the protrusions. Recently average roughness measurements were made by taking different profile samples from the cups and rotors. The results of these measurements are presented in Table 3.4.

Table 3.4 Results of Roughness Measurements

	Surface Type	Mean Roughness [μm]	Standard Deviation [μm]
Cups	Smooth	3.1	3.7
	Roughness # 1	13.0	15.6
	Roughness # 2	21.0	25.6
Rotors	Smooth	2.0	2.4
	Roughness # 1	38.0	45.5
	Roughness # 2	44.0	50.0

3.7 Results and Discussions

The viscosity of dynamic foam was tested using smooth and roughened cup-rotor assemblies. Measured shear stress readings were corrected using the calibration curves presented previously. Figure 3.11 shows foam rheology measurements obtained using the smooth cup-rotor assembly. Generally foam behaves like a shear thinning fluid and apparent foam viscosity increases with foam quality. Similarly, rheology measurements are presented in Fig. 3.12 that were obtained using roughened cup-rotor assembly (roughness No. 1). It is apparent from the figures that at a given shear rate the shear stress measured with the roughened cup-rotor assembly is considerable higher that the smooth assembly. This shows the presence of wall slip since the only difference between these two cup-rotor assemblies is their roughness.

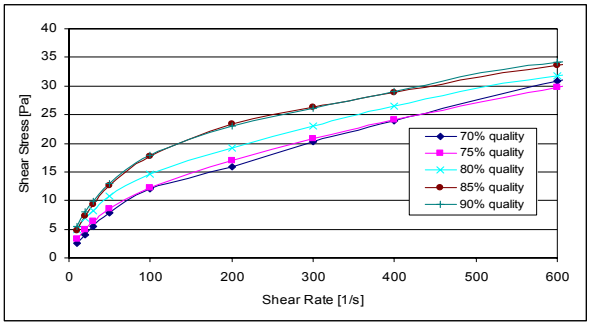

Fig. 3.11 Foam rheology measured using smooth cup-rotor assembly

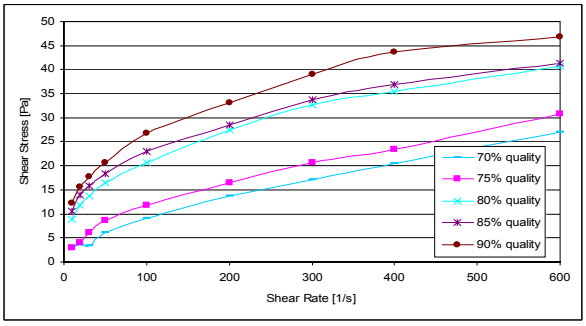

Fig. 3.12 Foam Rheology measured using roughened cup-rotor assembly (roughness No. 1)

It appears that measuring foam rheology with a smooth rotational viscometer underestimates the apparent foam viscosity; therefore measurements obtained using smooth and roughened cup-rotor assemblies are necessary to determine the wall slip effect and the correct rheology. Here the question is what level of roughness is sufficient to determine the wall slip. In order to get the effect of roughness on foam rheology, measurements were performed using a more roughened cup-rotor assembly (roughness no. 2). Figure 3.13 shows flow curves of foams measured using the more roughened cup-rotor assembly. The result shows that most of these measurements (i.e. shear stresses) are less than the measurements obtained using the other roughened cup-rotor assembly (roughness no. 1).

Figures 3.14 through 3.18 show the measured shear stress versus shear rate for a given quality foam. In each plot, there are three flow curves, representing rheology measurements obtained using the three different cup-rotor assemblies that have different surface roughnesses. At a given shear stress, a distinct difference in shear rate is observed. These variations could be due to the wall slip. For foam quality greater than 75%, measurements obtained using the most roughened cup-rotor assembly (roughness no. 2) is less than measurements with roughness no. 1. This is an unexpected result. In depth investigation of this phenomenon is necessary to present a more scientific reasoning to this observation.

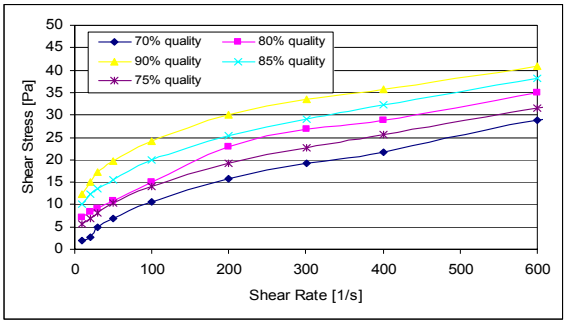

Fig. 3.13 Foam rheology measured using very rough cup-rotor assembly (roughness No. 2)

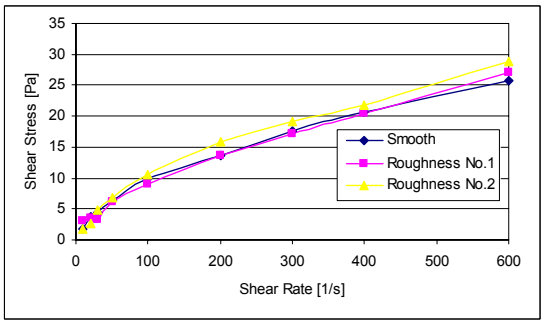

Fig. 3.14 Flow curves of 70% quality foam measured using different cup-rotor assemblies

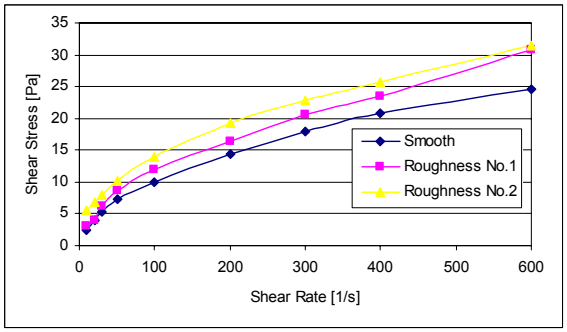

Fig. 3.15 Flow curves of 75% quality foam measured using different cup-rotor assemblies

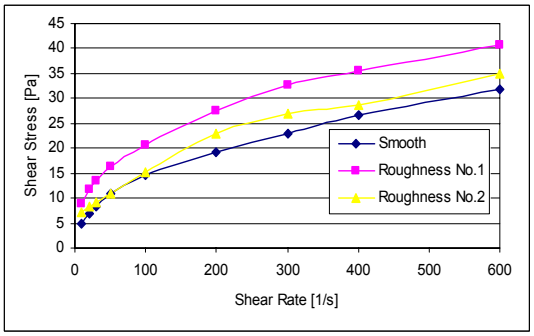

Fig. 3.16 Flow curves of 80% quality foam measured using different cup-rotor assemblies

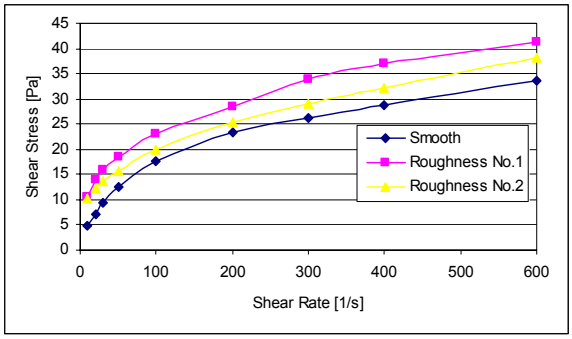

Fig. 3.17 Flow curves of 85% quality foam measured using different cup-rotor assemblies

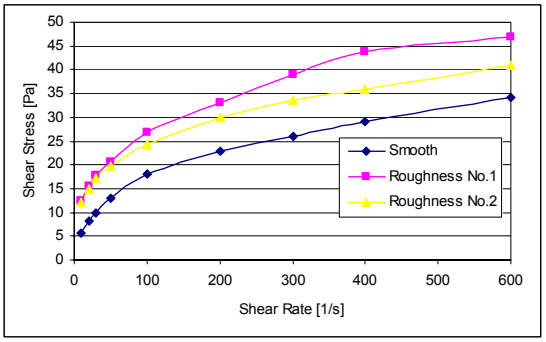

Fig. 3.18 Flow curves of 90% quality foam measured using different cup-rotor assemblies

For each foam rheology test, photographs of foams were captured through a view port using a microscope and a CCD camera. A Nikon SMZ800 microscope is aligned with a glass view port cell on the upstream of the RS 300 rheometer. A microscopic foam image was captured with the CCD camera attached to the microscope. The magnification scale of the microscope was 1:200. Figure 3.19 and 3.20 show two sample pictures of 70% and 90% quality foam. The evaluation of the average bubble size and investigation of the relationship between bubble size and foam rheology are in progress.

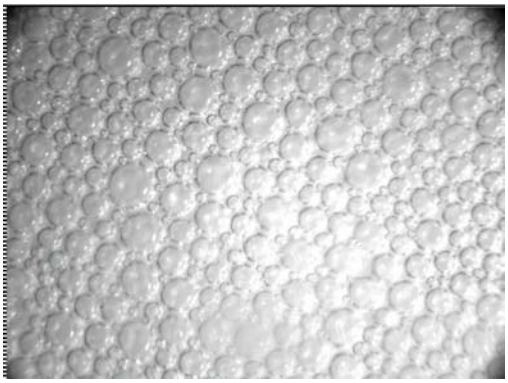

Fig. 3.19 Picture of 70% quality foam

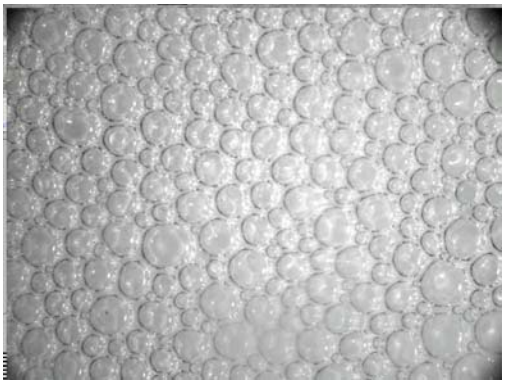

Fig. 3.20 Picture of 90% quality foam

4. STUDY OF CUTTINGS TRANSPORT WITH FOAM UNDER EPET CONDITIONS (TASK 13)

INVESTIGATOR: Zhu Chen (Ph.D. Candidate)

4.1 Introduction

This research task was not in the original proposal. It is a continuation of two other research tasks (Task #6 and Task #9) on foam rheology and cuttings transport. Literature survey, mathematical modeling, and preliminary rheology and cuttings transport tests are in their final stage. This task will extend beyond the 5-year DOE project timeline. It is scheduled to be completed in August, 2005.

The objectives of this project are: i) to investigate experimentally foam rheology under EPET conditions using pipe viscometers; ii) to determine experimentally volumetric requirements for effective cuttings transport with foam in horizontal wellbores without pipe rotation; iii) to develop a mechanistic cuttings-transport model; and iv) to verify the cuttings transport predictions of the model with experimental data.

4.2 Re-Calibrate Nuclear Densitometer

Re-calibration work for two nuclear densitometers has been finished. The densitometers were calibrated one year ago. At that time, the original plastic inner pipe in the annular section was replaced by thick-wall steel drillpipe. The reasons for re-calibration are mainly because of:

1. Reorientation of the densitometers (the nuclear source and the detector positions were reversed);
2. Low nuclear densitometer readings, which were observed during preliminary foam test;
3. Change in source intensity with time.

A calibration rig used for re-calibrating the densitometers is shown in Fig. 4.1. A 13-point calibration procedure was used to generate a calibration curve. This time more low-density points were added to measure foam density because more accurate data is required in the low-density range. Table 4.1 shows the mixture combinations that were used during the calibration process.

Recalibration was also performed with 1% surfactant foam. When the preliminary rheology tests were conducted, we were unable to measure foam density using the densitometers. During the re-calibration, we have found that when a linearization algorithm of the densitometer controller is turned off, low-density readings can be obtained from the densitometers. For the actual flow loop foam experiments, this still needs to be verified.

Fig. 4.1 Calibration rig

Table 4.1 Calibration Curve for Densitometers

Composition	Densitometer #1 (downstream)			Densitometer #2 (upstream)		
	Raw Counts	Measured SpG	True SpG	Raw Counts	Measured SpG	True SpG
100% air	37400	0.00	0.00	36723	0.00	0.00
5% water	36450	0.12	0.05	36045	0.084	0.05
10% water	35723	0.191	0.10	35370	0.163	0.10
15% water	35561	0.254	0.15	34817	0.234	0.15
20% water	34977	0.325	0.20	34226	0.305	0.20
25% water	34308	0.391	0.25	33917	0.375	0.25
50% water	32248	0.635	0.50	31808	0.629	0.50
75% water	30917	0.837	0.75	30592	0.801	0.75
100% water	28465	1.213	1.00	28306	1.18	1.00
25% cuttings+water	26954	1.45	1.248	26296	1.46	1.248
50% cuttings+ water	25676	1.655	1.497	25372	1.627	1.497
75% cuttings +water	24501	1.841	1.744	24336	1.795	1.744
100% cuttings+ water	23797	1.99	1.992	23318	1.992	1.992

Figure 4.2a shows the calibration curve for densitometer #1. From this curve, each time a measured density is read, the polynomial regression formula in the LabView system will be used to convert the measured value into the true actual density. Compared with previous calibration data, the number of raw counts is slightly decreased. However, the relative change in source intensity is negligible. Calibration results of the densitometers are presented in Fig. 4.2b in the form of ratio of the actual to measured specific gravity vs. the

measured specific gravity. At higher specific gravities (i.e. greater than 0.4) the calibration curves of the densitometers have approximately the same pattern; but they are considerably different at low specific gravities.

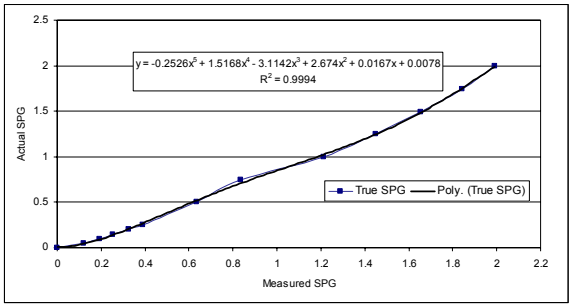

Fig. 4.2a Calibration curve for densitometer #1

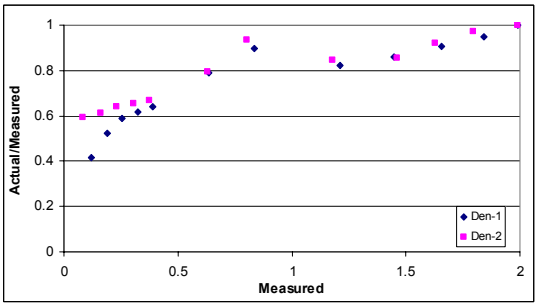

Fig. 4.2b Ratio of actual to measured SpG vs. measured SpG

4.3 Cuttings Injection System Installation and Testing

A multiphase cuttings injection system (Moyno progressive cavity pump) was installed at the bottom of the injection tower. It replaced the previous injection auger. The new cuttings injection multiphase system, as shown in Fig 4.3, is capable of injecting cuttings at the required rate. Table 4.2 shows the initial test results of the injection rate and pump rotational speed; it can be seen that a controllable injection rate is achieved.

Fig. 4.3 Cuttings injection system

Table 4.2 Injection Rate and Rotational Speed for the Cuttings Injection System

Cuttings Injection System Rotation Speed (RPM)	20	40	60
Rate of Change of Injection Tower Weight (lb/Min)	6.0	9.0	14.1
Rate of Change of Removal Tower Weight (lb/Min)	4.2	9.4	10.5
Injection Rate [lb/Min]	9.6	14.4	22.6

4.4 Installation and Test of Other ACTF Systems

The major construction project during this quarter is to dismantle the previous annular test section, to mount the annulus and 4" pipe on a mast, and to install two hydraulic cylinders to elevate the mast and test section. The mast is about 10' above ground. By the time this report is written, mechanical and electronic modifications will have basically been completed. Water and water cuttings tests have been performed. Also, the flow loop elevation system has been tested. The pipe rotation system has been tested up to 200 RPM. A new recirculation line has been installed, and it allows foam to be recirculated from the return line to the multiphase Moyno pump. A large Sullair air compressor was installed, and it can operate at 500 psi and 900 cfm maximum flow rate. Flexible hoses have been hooked up to the injection tower and removal tower. The weighing systems for the injection and removal towers have been tested. All transducers have been installed and the final Labview control system is ready to operate.

5. STUDY OF CUTTINGS TRANSPORT WITH AERATED MUD UNDER EPET CONDITIONS (TASK 10)

INVESTIGATOR: Lei Zhou (Ph.D. Candidate)

5.1 Objectives

- Develop two-phase flow model for aerated fluids under elevated pressure and temperature conditions inside an annulus in a horizontal position without pipe rotation.
- Determine experimentally the cuttings transport ability of aerated fluids under elevated pressure and temperature conditions.
- Determine the gas/liquid flow rates for effective cuttings transport.
- Develop a computational tool to calculate pressure loss in aerated fluids flowing under elevated pressure and temperature conditions.

5.2 Comparison of Model Predictions with the Measured Data

A mechanistic model for cuttings transport with aerated mud has been developed. The hydraulics of one-dimensional, two-phase (gas-liquid) flow is coupled with the mechanisms of cuttings transport in the formulation of the model. The model determines the flow pattern and predicts the in-situ cuttings concentration, mixture density and frictional pressure losses in a horizontal concentric annulus. Details of the mechanistic model were described in the last DOE quarterly report. Cuttings transport mechanisms with aerated water at various conditions (different air and water flow rates, different pressures and temperatures) were investigated. A total of 39 tests were performed. Table 5.1 (see Appendix) shows the test pressures and temperatures for each test group. The base case (Test Group #1) includes 16 tests. Other test groups include: 8 low temperature tests, 8 high temperature tests and 7 high temperature and high pressure tests. Pressure and temperature were varied to maintain a constant gas-liquid ratio (GLR). For each group, tests were performed at four different GLRs (0.0, 0.12, 0.24, and 0.38). At high GLRs (i.e. greater than 0.38), the flow loop became mechanically unstable. Therefore, GLRs greater than 0.38 were avoided for safety reasons. Detailed results of all the test groups are presented in Tables 5.2 to 5.5 in the Appendix.

Measured cuttings concentrations for the base case (Test Group #1) are presented along with the model predictions in Table 5.2. The absolute average differences between measured and predicted cuttings concentrations at liquid flow rates of 80, 100, 120 and 150 gal/min are 13.45%, 12.54%, 12.67% and 22.06%, respectively. For 150 gal/min water flow rate, the absolute average difference is the highest (i.e. 22%) because at high liquid flow rates the cuttings concentration is low. Hence, test measurement relative error can be higher than at low liquid flow rate tests. The overall absolute average difference for the base case is 15.2%. In addition to the liquid flow rate, GLR affects the accuracy of the model predictions. It appears that the model accuracy decreases with increasing GLR.

Figures 5.1 and 5.2 compare cuttings concentration predictions of the model together with experimentally measured data for low temperature tests (Test Group #2). For this set of tests the model predictions are very close to the measured data. For instance the model predictions at 100 gal/min liquid flow rate show only 10% absolute average difference. At 120 gal/min liquid flow rate, the absolute average difference becomes 22%. The overall absolute average difference for the group is 16%.

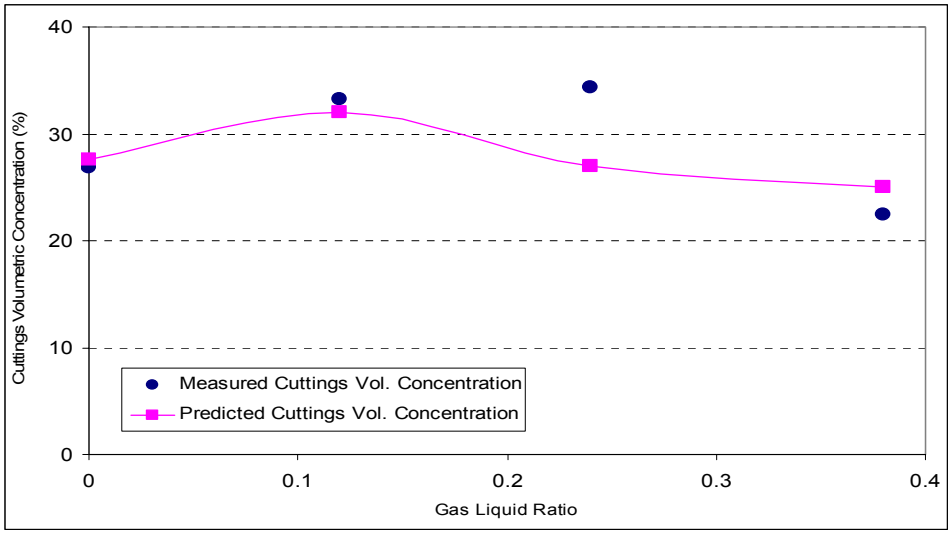

Fig. 5.1 Measured and predicted cuttings concentrations vs. GLR (QL=100 gal/min, T =80°F, P=185 psi)

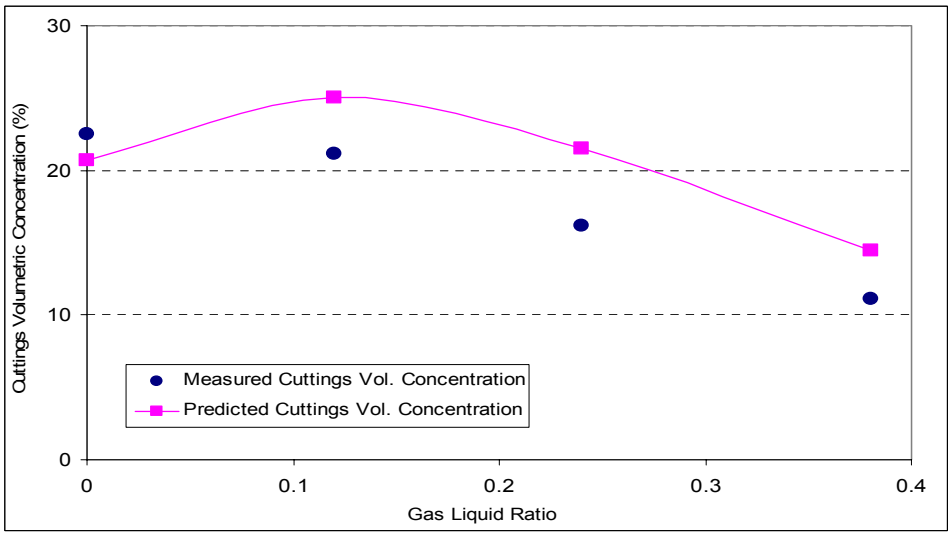

Fig. 5.2 Measured and predicted cuttings volumetric concentration vs. GLR (QL=120 gal/min, T =80°F, P=185 psi)

For high temperature tests (Test Group #3), the model predictions have an absolute average difference of 30% at liquid flow rate of 100 gal/min. At 120 gal/min liquid flow rate, the absolute average difference is 35%. The overall absolute average difference for high temperature tests is 32%. The increase in discrepancy between the measured and predicted

values may be attributed to the use of empirical equations that are obtained from ambient temperature two-phase flow experiments. Figures 5.3 and 5.4 present cuttings concentration predictions of the model together with experimentally measured data for high temperature and pressure tests (Test Group #4).

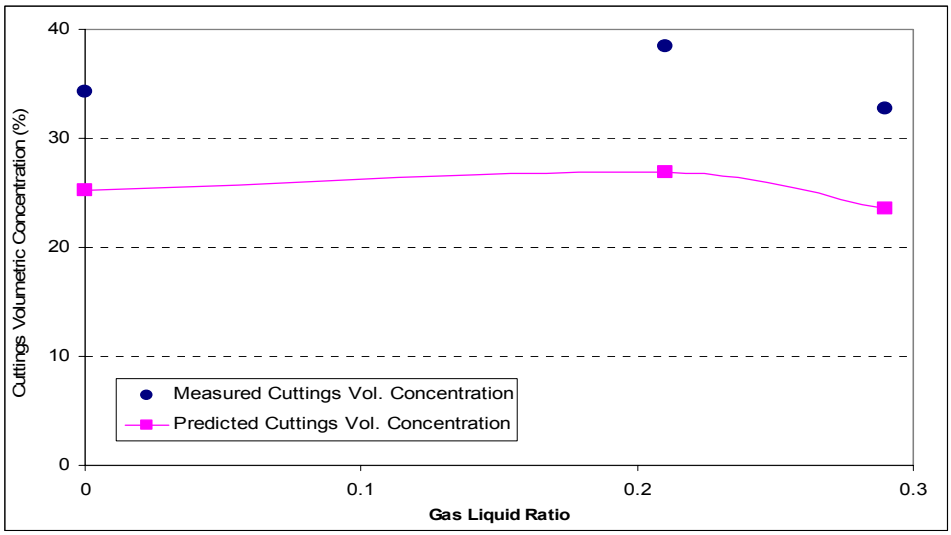

Fig. 5.3 Measured and predicted cuttings volumetric concentration vs. GLR (QL=100 gal/min, T =175°F, P= 500 psi)

As shown in the figures, the model predictions follow the trends of the experimental data, but underestimate the cuttings concentration. For this test group, the model gives an absolute average difference of 28% at liquid flow rate of 100 gal/min. At higher liquid flow rate (120 gal/min), the absolute average difference is 34%. The overall absolute average difference for this test group is 30%.

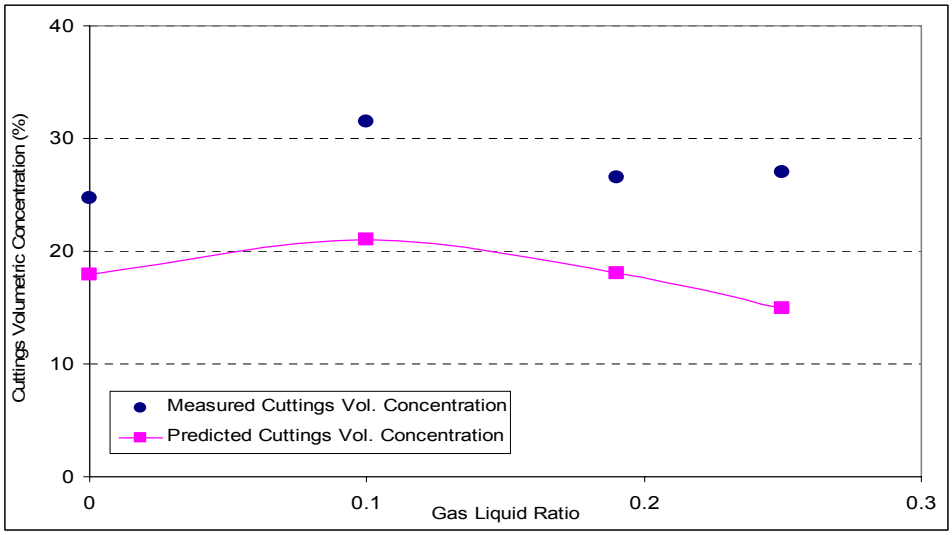

Fig. 5.4 Measured and predicted cuttings volumetric concentration vs. GLR (QL=120 gal/min, T =175°F, P= 500 psi)

5.3 Delivered

1. Semi-annual Advisory Board Meeting (ABM) reports;
2. Two-phase flow model for aerated fluids under elevated pressure and temperature conditions;
3. Experimental data base for aerated mud cuttings transport under EPET conditions;
4. Practical guidelines and/or graphs to determine the gas/liquid rate for effective cuttings transport capacity under elevated pressure and temperature conditions;
5. A computational tool to calculate frictional pressure drops inside an annulus for aerated fluids flowing over the range of experimental conditions.

Appendix

Table 5.1 Test Parameters of Cuttings Transport Experiments

	Group Identification	Number of Tests	P (psi)	T (°F)
Group #1	Base case	16	200	120
Group #2	Low Temperature	8	185	80
Group #3	High Temperature	8	220	170
Group #4	High Temperature & Pressure	7	500	175

Table 5.2 Model Predictions and Measured Data for the Base Case (P=200 psi, T =120 °F)

QL =80 gal/min			
GLR	Measured Vol. Concentration (%)	Predicted Vol. Concentration (%)	Absolute Difference (%)
0	42.02	37.6	10.52
0.12	38.20	39.0	2.09
0.24	40.80	34.0	16.67
0.38	42.40	32.0	24.53
Average Absolute Difference (%)			13.45
QL =100 gal/min			
GLR	Measured Vol. Concentration (%)	Predicted Vol. Concentration (%)	Absolute Difference (%)
0	28.42	26.00	8.52
0.12	28.42	29.40	3.45
0.24	30.56	27.50	10.01
0.38	31.48	22.60	28.21
Average Absolute Difference (%)			12.54

QL =120 gal/min			
GLR	Measured Vol. Concentration (%)	Predicted Vol. Concentration (%)	Absolute Difference (%)
0	19.63	19.10	2.70
0.12	20.17	22.50	11.55
0.24	25.67	18.00	29.88
0.38	11.77	11.00	6.54
Average Absolute Difference (%)			12.67
QL =150 gal/min			
GLR	Measured Vol. Concentration (%)	Predicted Vol. Concentration (%)	Absolute Difference (%)
0	10.16	9.6	5.51
0.12	8.63	10.0	15.87
0.24	6.49	5.0	22.96
0.38	5.35	3.0	43.93
Average Absolute Difference (%)			22.06

Table 5.3 Model Predictions and Measured Data for Low Temperature Tests

QL =100 GPM			
GLR	Measured Vol. Concentration (%)	Predicted Vol. Concentration (%)	Absolute Difference (%)
0	26.89	27.60	2.64
0.12	33.31	32.15	3.48
0.24	34.38	27.5	20.01
0.38	22.46	25.05	11.53
Average Absolute Difference (%)			9.42
QL =120 GPM			
GLR	Measured Vol. Concentration (%)	Predicted Vol. Concentration (%)	Absolute Difference (%)
0	22.46	20.70	7.84
0.12	21.16	25.05	18.38
0.24	16.20	21.50	32.72
0.38	11.15	14.50	30.04
Average Absolute Difference (%)			22.25

Table 5.4 Model Predictions and Measured Data for High Temperature Tests

QL =100 GPM			
GLR	Measured Vol. Concentration (%)	Predicted Vol. Concentration (%)	Absolute Difference (%)
0	36.37	24.00	34.01
0.12	35.37	27.00	23.66
0.24	33.46	26.50	20.80
0.38	33.54	20.00	40.37
Average Absolute Difference (%)			29.71
QL =120 GPM			
GLR	Measured Vol. Concentration (%)	Predicted Vol. Concentration (%)	Absolute Difference (%)
0	20.63	17.00	17.60
0.12	24.68	20.00	18.96
0.24	25.06	16.00	36.15
0.38	29.26	10.00	65.82
Average Absolute Difference (%)			34.63

Table 5.5 Model Predictions and Measured Data for High Temperature and Pressure Tests

QL =100 GPM			
GLR	Measured Vol. Concentration (%)	Predicted Vol. Concentration (%)	Absolute Difference (%)
0	34.23	25.20	26.37
0.21	38.43	26.87	30.08
0.29	32.70	23.57	27.92
Average Absolute Difference (%)			28.12
QL =120 GPM			
GLR	Measured Vol. Concentration (%)	Predicted Vol. Concentration (%)	Absolute Difference (%)
0	24.68	17.88	27.55
0.1	31.48	21.00	33.28
0.19	26.59	18.05	32.11
0.25	26.97	15.00	44.38
Average Absolute Difference (%)			34.33

6. DEVELOPMENT OF CUTTINGS MONITORING SYSTEM (TASK 11)

INVESTIGATORS: Kaveh Ashenayi and Gerald Kane

6.1 Objective

The ultimate objective of this task (Task 11) is to develop a non-invasive technique for quantitatively determining the location of cuttings in the drill pipe. Four different techniques were examined. However, as pointed out in previous reports an ultrasound method showed good potential for success and was chosen.

6.2 Team Composition

The instrumentation team charged with completing tasks 11 consisted of Dr. Gerald R. Kane and Dr. Kaveh Ashenayi both registered professional engineers and professors of Electrical Engineering Department at the University of Tulsa. MS level graduate students are assisting them. These students have BS degrees in EE and CS. This particular combination works well because successful completion of this project requires skills needed in both disciplines. To achieve objectives of this task we will need to develop a very complicated electronic hardware/sensor and a software package that correctly interprets the data received. In addition, Mr. Len Volk is a member of this team working on task 12.

6.3 Progress to Date

We conducted static and dynamic tests to see if the basic system is functioning correctly. We used the DTF test facility to evaluate system's response. The system did indicate different sand levels by providing a unique number. As sand was added the system response changed.

While performing the tests, we observed that for getting consistency in performance it is necessary to secure the sensors in the caps in a particular way every time. Slight variation in position causes inconsistency in performance. To achieve this consistency we tried many methods of physically supporting the sensors in place. After many such trials we devised a secure and repeatable way of positioning the sensors in the cap 'exactly the same way every time' by devising inserts with threads and rubber washers for cushioning.

The data collection software revision is proceeding. The software will start by allowing the user to setup the communication characteristics of the system. Then it will proceed to identify the number of boards connected. The data received from the sensor board is in the form of ASCII characters. We developed and tested the conversion algorithm that allows us to calculate the numerical voltage value corresponding to the character combinations that are received. We have revised the software and the firmware for higher precision and accuracy.

The data processed by the software will be exported as a text file to be used as input for the neural network development package we purchased. We have been working with the software and we developed a large number of neural networks.

Using the screens and wire framework for achieving consistent cuttings bed height and the devised sensor-positioning scheme we have performed static and dynamic tests under low-pressure conditions on the DFT test facility. The test data is gathered and processed by the software and is stored and managed by using MS Access. We have trained many neural networks using Thinks Pro Neural Networks Version 1.05 for these static and dynamic tests.

For training the neural network we have used different architectures and configurations of the network along with different preprocessing techniques for the input data. We also have used different transfer functions for the hidden layer and output layer of the network. For input data we have considered differences of the readings as cuttings bed height is increased in 1" increments with respect to readings for no sand condition. Using consecutive cuttings bed height differences we generated a different data set. In this case we used differences between the successive 1" increase in cuttings bed height. We have used both normalized and non-normalized input data for training. For testing the trained neural networks we have used different data sets acquired during the static and dynamic tests performed. Table 6.1 shows a summary of the results obtained from trained neural networks for different test data.

Table 6.1 Summary of the Results Obtained From Trained Neural Networks

Training Set	Testing Set	Transfer Function	Nodes in hidden layer	Classification
1961OPD0	2561OPD0	Sigmoid Bipolar	8	68.00%
2561OPD0	1961OPD0	Sigmoid Bipolar	8	70.00%
1961OPD0	2561OPD0	Sigmoid Bipolar	6	71.00%
2561OPD0	1961OPD0	Sigmoid Bipolar	6	68.00%
1961OPD0	2561OPD0	Sigmoid Bipolar	4	76.00%
2561OPD0	1961OPD0	Sigmoid Bipolar	4	66.00%
1961OPDC	2561OPD0	Sine Bipolar	8	89.00%
2561OPDC	1961OPD0	Sine Bipolar	8	89.00%
1961OPDC	2561OPDC	Sine Bipolar	6	80.00%
2561OPDC	1961OPDC	Sine Bipolar	6	80.00%
1961OPDC	2561OPDC	Sine Bipolar	4	92.20%
2561OPDC	1961OPDC	Sine Bipolar	4	88.00%
1961OPD0	2561OPD0	Sigmoid Bipolar	8	68.00%
2561OPD0	1961OPD0	Sigmoid Bipolar	8	70.00%
1961OPDC	2961OPDC	Sine Bipolar	4	19.44%
1961OPD0	2961OPD0	Sigmoid Bipolar	4	50.00%
1963OPDC	2563OPDC	Bipolar	4	70%
2563OPDC	1963OPDC	Bipolar	4	59%
F2961OPDC	F2161OPDC	Sine Bipolar	4	44%
F2961OPDC	F2161OPDC	Sine Bipolar	8	45%
N1963OPD0	N2563OPD0	Sine	4	50%

The nomenclature used for identifying different networks is as shown in Fig. 6.1.

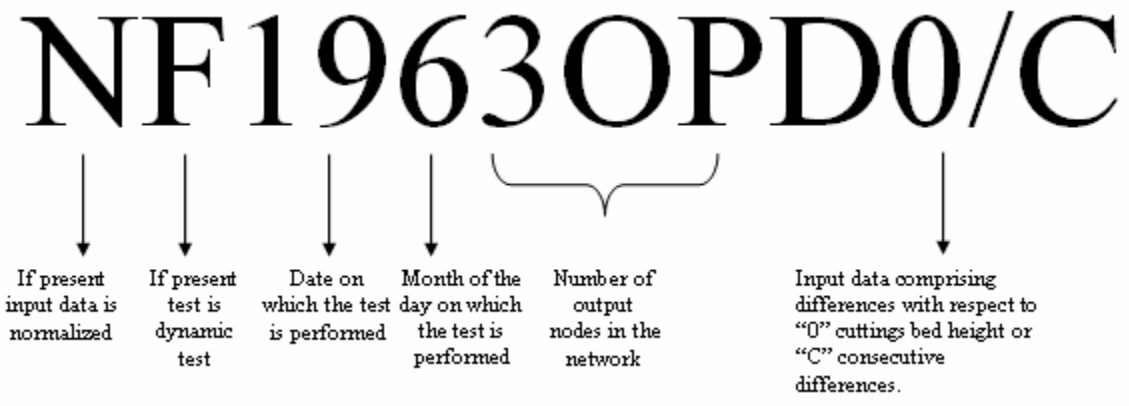

Fig. 6.1 Neural network nomenclature

Development of neural network is still continuing. We are developing new pre and post processing techniques. We finalized the board design and ordered the final control boards. We are still working on developing a solution for a potential problem with the sensors' impedance identified before. It seems that all units are not a close match from an impedance point of view. This could be a problem if we need to replace a sensor after the system has been calibrated. We are further investigating this problem.

A preliminary test was conducted on the main flow loop at 100 gpm flow rate and 20 lb/min cuttings injection rate. The measured bed thickness using ultrasonic method showed a satisfactory agreement with nuclear densitometer readings. The test involved installing two rings of sensors. We then proceeded and calibrated the sensors. This process was repeated several times due to different mechanical failures. The following outlines some of the reasons. We had a cap that was leaking and that put the unit into saturation. Long untwisted wire acts as an antenna and picks up stray RF signals. We had another cap that was sheared so it was not sitting flat. We had to replace wires due to the length effect on the value read. After we calibrated the sensors, we started to collect data. We collected a total of thirty different data points. These were collected after the test section was put in liquid hold mode. Readings indicated 2.5 to 2.7 inches of sand. The corresponding nuclear densitometers readings were between 2.5 and 3.1 inches.

Computer code has been implemented in Visual Basic to control the ultrasonic circuit board. This code has been tested during the ACTF flow tests in this phase. Data collected by this computer program from the ACTF flow tests was stored in a database for further analysis. This program runs on the in-line computer on the ACTF and communicates with the central computer using a "Dataserver" (National Instrument) through a fast (108M) wireless connection.

6.4 Approach

In subtask one of Task 11 we are to develop a static (followed by a dynamic) radial test cell and to develop a preliminary set of instruments to detect presence of cuttings in these cells. The main approach to be investigated is ultrasound transmission. We investigated the need for an inner ring.

7. FOAM BUBBLE CHARACTERIZATION METHOD (TASK 12)

INVESTIGATOR: Leonard Volk

7.1 Introduction

Bubbles (as foam or aerated fluid) will be moving at a high rate (up to 6 ft/sec) in the drilling section of the ACTF, and may be very small (down to 0.01 mm). The bubble size and size distribution influence the fluid rheology and the ability of the fluid to transport cuttings. Bubbles in a shear field (flowing) may tend to be ellipsoidal which might alter both the rheology and transport characteristics.

This project is Task 12 (Develop a Method for Characterizing Bubbles in Energized Fluids in the ACTF During Flow) in the Statement of Work, and is divided into four subtasks:

- Subtask 12.1. Develop/test a microphotographic method for static conditions
- Subtask 12.2. Develop/test a method for dynamic conditions
- Subtask 12.3. Develop simple, noninvasive methods for bubble characterization
- Subtask 12.4. Provide technical assistance for installation on ACTF

Subtask 12.1 includes (1) magnifying and capturing bubble images, (2) measuring bubble sizes and shapes, and (3) calculating the size distribution and various statistical parameters. Subtask 12.2 develops the methods needed to apply the results of Subtask 12.1 to rapidly moving fluids, especially the method of "freezing" the motion of the bubbles. A dynamic testing facility will be developed in conjunction with Task 11 for development and verification.

Subtask 12.3, added in year 3, develops simple, inexpensive and small-in-size methods for characterizing bubbles. This task was previously referred to as "New Techniques".
Techniques and methods developed under Subtasks 12.2 and 12.3 will be applied to the drilling section of the ACTF in Subtask 12.4.

The objective of this task is to develop the methodology and apparatus needed to measure the bubble size, size distribution and shape during cuttings transport experiments.

7.2 Monitoring On-Line Non-Intrusive Measurement Systems

Three on-line measurement systems, ultrasonic system, CCD camera system and the flow cart, will be installed on the ACTF flow loop. The ultrasonic system will be used to measure local cuttings concentration. The on-line CCD camera system will be used to take pictures of the test section through view ports. The flow cart will be used to take a real fluid sample from the test section and perform a detailed fluid characterization test.

7.2.1 On-Line Vision System

The objectives of the on-line vision system are: i) to obtain dynamic bubble images from the cart system; and ii) to acquire real-time flow images using the CCD camera installed on the view-port. Images taken by the CCD camera will be transferred by the on-line computer to the control room during the experiments. A computer will be installed on the ACTF flow loop to control the CCD camera system and to communicate with a central computer in the control room. Dynamic bubble images obtained from the cart will be used for determining the bubble size distribution. It is well documented that foam texture has strong effects on foam rheology. Therefore, foam characterization is very import for cuttings transport.

A picture showing a setup of on-line system is shown in Fig. 7.1. The CCD camera (Hitachi KP F-120 CL progressive scan with 1.45M pixels, see Fig. 7.2) was installed close to the view port (Fig. 7.3) to capture real-time images. A camera link grabber (National Instruments PCI-1428) was installed on the in-line computer and connected to CCD camera through a 2-meter camera link cable. The camera link grabber was used to process the signals obtained by the CCD camera.

Fig. 7.1 On-line vision system

In order to obtain good quality images, a light source is needed because the test section is completely dark during the tests. An adjustable light source was used in the system to provide the desired light. Two type of light source, a fiber light source (Fig. 7.4) and a ring light source (Fig. 7.5), were used and tested in the system to identify the best light source that can be used on the ACTF flow loop. Both light sources have their own light intensity controller. The ring light source has a controller that can be connected to a computer through RS-232C serial port. The in-line computer controls the intensity of the ring light through a RS-232 C port using a computer program. By carefully adjusting the light source through the controller, a sharp image of the test section can be obtained through the view port as shown in Fig. 7.6. When used on the flow loop to take real-time images, data can be stored on the in-line computer or transferred to the control room through a fast (108M) wireless network connection.

Fig. 7.2 CCD Camera together with Lens

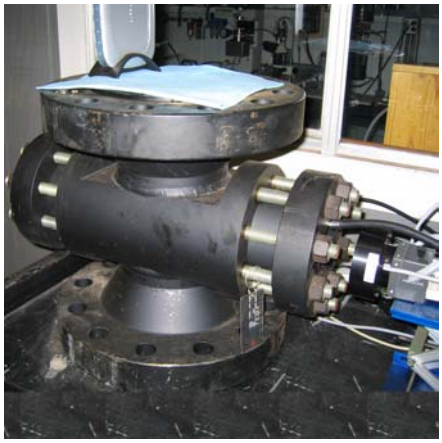

Fig. 7.3 View port

Computer codes have been implemented in C++ for capturing the image. Two operations can be performed through the program: 1) Snap a still image; 2) Grab continuous images (video). The program can acquire still images and/or the dynamic video during the test. A still image can be obtained whenever needed using the program developed in this phase. Recently, the image program has been used in the foam Generator/Viscometer test (Task 9b). Using the still images obtained by the program, bubble size distribution can be analyzed by Particle 2.0 (the software presented in the last report). The program can record dynamic videos at the rate of 15 frames per second.

Fig. 7.4 Fiber light with the controller

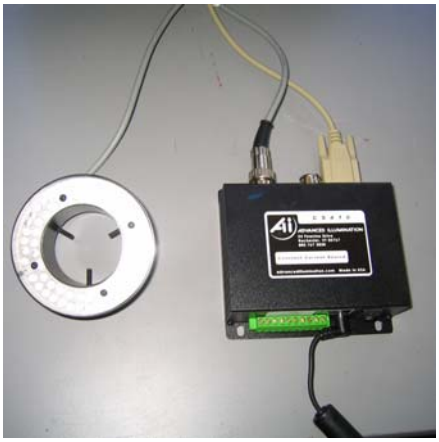

Fig. 7.5 Ring light and controller

Lab tests were conducted to check the on-line vision system. Sharp images were obtained through the CCD camera with the use of the ring light or the fiber light. Figure 7.7 shows the picture of CCD camera with both light sources (Fiber light and Ring light) installed. Preliminary results indicate that fiber light provides a better image while ring lights show reflection problems. During the lab tests, it was found that up to 15 frames per second can be achieved when grabbing continuous images. The “Client-Server” control system was tested in the lab. Tests results showed good response rate.

Fig. 7.6 Image of cuttings in the test section

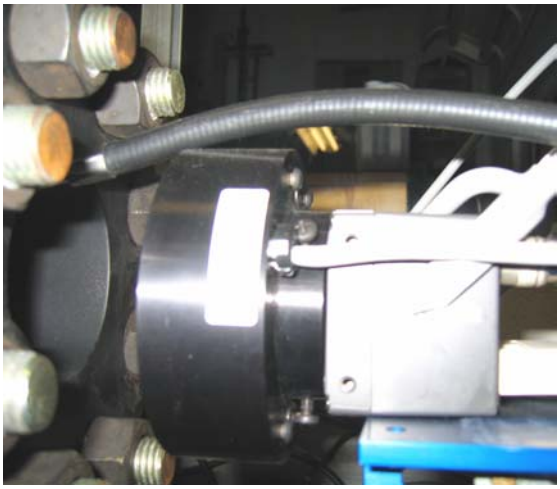

Fig. 7.7 CCD camera with fiber light and ring light installed

7.2.2 Synchronization of On-Line Measurement Systems

Synchronization of sub systems (on-line vision system, Ultrasonic system and flow cart dynamic bubble characterization system) is very important to control and manipulate the streams of sampled data and images. In order to synchronize the sub systems, a distributed system with a “Client-Server” structure has been developed. All on-line sub systems are “linked” through a wireless network to communicate with the central computer. Initially, all sub systems listen to a “socket”. They will be blocked when there is no message available on that socket. The central computer located in the control room can trigger all the on-line sub systems when tests are started by broadcasting (sending) a message to them.

7.3 Novel Techniques for Bubble Characterization

Figure 7.8 shows a prototype of the device for measuring the average bubble size for the foam generator-viscometer. This prototype is constructed from a ½” fitting. Light is supplied by a white light-emitting diode (LED) shown at the top of the photo, and the transmitted light is recorded by a photodiode, located in the fitting shown removed. Both the LED and photodiode are separated from the foam by small glass windows.

Fig. 7.8 Prototype device for measuring the average bubble size of foam

7.4 Installation of Bubble Characterization Methodology on ACTF

The new windowed cell has been received and installed on the ACTF Bubble Characterization Cart (the Cart). The cell is designed to:

1. Eliminate the dead volume that occurs in standard windowed flow-through cells
   Advantage: As foam quality increases, foam flow becomes laminar, which causes static foam to reside next to the viewing window. This static foam is no longer representative of the bulk foam.
2. Allow better illumination of flowing foam
   Advantage: Beveling the window retainer at 45° and increasing the exposure on either side of the flow channel increases the light intensity and uniformity, which helps imaging and subsequent processing for calculating the bubble size distribution.
3. Maintain a nearly uniform cross-section to flow through the cell
   Advantage: A uniform cross section prevents radical changes in pressure, which in turn reduces the alteration of the bubble size distribution.

Figure 7.9 is a picture of the installed cell. The overall cell has a diameter of 5". The window opening is 1.2" in diameter and the glass is 0.5" thick. The flow channel is 0.52" wide by 3/8" deep. The ½" tubing fittings have been drilled out to allow the tubing to pass through to help maintain a uniform flow cross section.

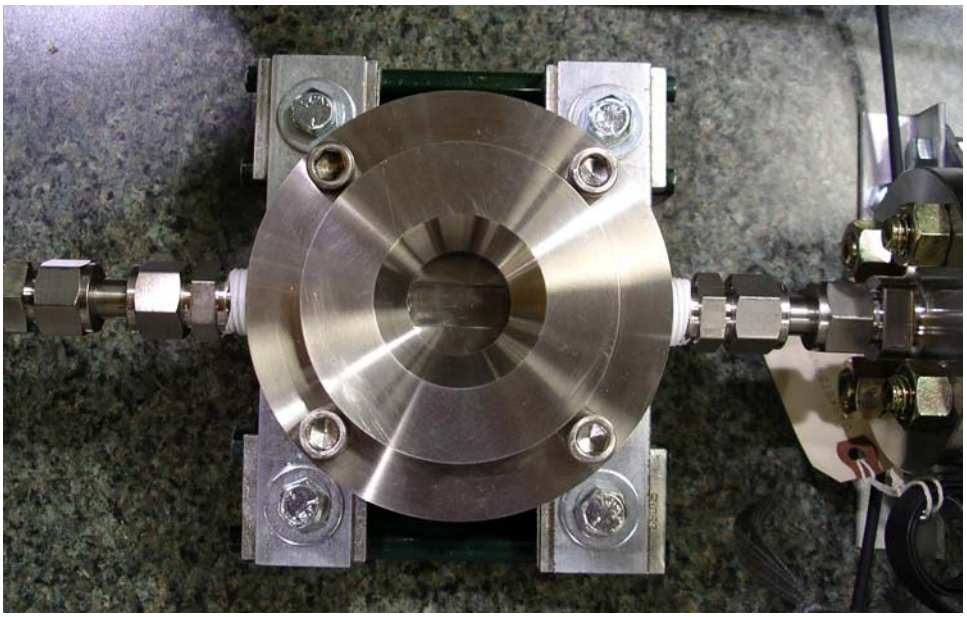

Fig. 7.9 Windowed flow cell installed on ACTF bubble characterization cart

Figure 7.10 is an overall photograph of the Cart without the Lexan top or aluminum side panels. Foam flow is from left to right. The tall structure at the left near the point of fluid entrance is the pressure relief valve, set at 700 psi, the maximum working pressure of the Cart. The electrically-actuated valves (under yellow boxes) serve to briefly stop and isolate the foam for microphotography. A long focal length microscope equipped with a digital camera captures foam in the windowed cell. After leaving the windowed cell, the foam flows

through a magnetic flow meter and past the pressure and temperature transducers (hidden behind the large red control valve). After passing through the second electrically-actuated ball valve (yellow box), the foam can either be directed though a manually operated needle valve or electrically controlled variable orifice (large red cylinder). These serve to control the rate of fluid flow and maintain the system pressure at nearly the same pressure as in the ACTF to which the Cart is attached with a high-pressure flexible metal hose.

The CPU and computer monitor are shown below the instrumentation platform. The computer is connected to the electrical components on the instrumentation platform through the data acquisition system, shown mounted vertically just inside the right rear corner of the Cart next to the monitor. Communication between the Cart and the Control Room is done wirelessly. Roll-out shelves help access to the CPU and monitor. Large, heavy-duty 6" wheels allow the Cart to be moved into place at several monitoring stations on the ACTF. Once in place, floor jacks can be activated to stabilize the Cart.

Fig. 7.10 ACTF bubble characterization cart

8. SAFETY PROGRAM (TASK 1S)

Chairman, Process Hazards Review Team: Leonard Volk

8.1 Introduction

This project was initiated during the fourth quarter of 2000 to assess the hazards associated with the Advanced Cuttings Transport Facility (ACTF) and develop an Action Plan to address problems discovered during this Hazards Review. A Hazards Review is an industry accepted method used to improve the overall safety characteristics and reduce the possibilities of accidents in the work place. Each individual component of the ACTF is examined as to the effect and consequences on safety, health, and the environment, of the component in all possible operational modes. A Hazards Review can result in equipment modification, inspection and testing, documentation, personal protective equipment, personnel training, and/or emergency training. The hazards review process begins by selecting a review method. Next a team of qualified individuals must be formed. This team should include those knowledgeable in the review process and those familiar with the process to be reviewed. Prior to beginning the review, all available documentation needs to be gathered. This includes schematics, organized training, periodic inspections and testing results, design and construction documents, operating procedures, etc. Once the schematics have been verified and the operator of the equipment or process has reviewed its operation with the team, the Hazards Review begins. The review should continue uninterrupted until completed. After the findings and recommendations have been completed, a draft report is issued and reviewed by all team members, and the operator of the process or equipment. Following this review, any changes are incorporated and a final report issued. This completes the Hazard Review process. The operator then needs to develop an action plan to implement the recommendations from the Hazard Review. In our case, team members will participate in developing this plan.

8.2 Objective

The objective of this task is to identify problems (findings) that might result in injury, property damage or the release of environmentally damaging materials and provide recommendations to minimize them, and to develop an action plan based on these recommendations.

8.3 Project Status

Signing has been added and, shortly, isolation chain will be installed around the facility. Once the final construction has been completed on the ACTF, operational schematics will be drawn as a prelude to a Hazards Review of the facility. During the third quarter of 2003 (Year 4), a table labeled “Hazards Review Finding Status” was developed to track the progress in resolving the various Findings. Tables 8.1 presents the current status as reported by Mark Pickell and Steve Turpin.

Table 8.1 Current Status of Hazards Review Findings (7-01-04)

Finding		Response	Completed
1	No monitoring of a "no flow" condition of pump while operating	Enabled alarms in LabView program to indicate a failure when flow level is at a zero flow condition	100%
2	No design documentation for piping or fittings	Drawings and Technical Documentation book completed	100%
3	No design documentation for relief valves	Document template completed. Data input in progress.	20%
4	No inspection documentation for relief valves	Document template completed. Data input in progress	20%
5	Insufficient splash protection	Splash guards installed	100%
6	Improper hose for application	Suction piping re-built & hose replaced	100%
7	No design documentation for hose	Drawings and Technical Documentation book completed	100%
8	No inspection procedure & documentation for hoses	Document template completed	10%
9	Incorrect relief valve pressure setting	Relief valve settings re-set	100%
10	No pressure bleed valve	A new valve was installed to allow the pressure to bleed into the process piping	100%
11	Air hose not secured	Air hose removed; hook-up for stainless steel tubing installed	100%
12	No Reverse flow protection	Changed piping configuration to eliminate the possibility of reverse flow	100%
13	No relief protection	This is a return line from the fuel supply on the low pressure diesel pump no relief is required	100%
14	Incomplete design documentation of components (valves, etc)	Drawings and Technical Documentation book completed	100%
15	No written operating procedure	Students now required to write operating procedures for their experiments	100%
16	Improper direction of released fluid	Installed deflection shield and directed air blast in a safe direction	100%
17	Inadequate protection against high-volume gas release	Relief discharges piped beneath splash guards or elevated	100%
18	Flammable material too close to ignition source	New fuel tank installed	100%
19	No Secondary spill containment	Moved Diesel Tank into the confines of the containment trenches	100%
20	No placarding or labeling of containers or equipment storing flammable or hazardous material	Signage in place	100%
21	Tubing incompatible with contents	Removed from diesel tank	100%

Finding		Response	Completed
22	No protection against mechanical breakage-diesel site tube	Removed from diesel tank	100%
23	No automatic shut off fuel supply	Moved Diesel Tank into the confines of the containment trenches	100%
24	Inadequate number / location of fire extinguishers	Three additional fire extinguishers have been purchased and received / awaiting installation	80%
25	No site-specific emergency action plan	Building Emergency Plan adopted; further review needed to be site specific for the test loop	80%
26	No specific lock-out, tag-out procedure	Lock-out, tag-out training courses completed by personnel	100%
27	No corrosion inspection procedure & documentation for corrosion	Ultrasonic thickness gage purchased and received / a regular and documented inspection schedule yet to be implemented	60%
28	No written operating procedure	Students now required to write operating procedures for their experiments	100%
29	No documented training procedure for operating personnel	Safety training documented and maintained	100%
30	No documented safety training program	Safety training documented and maintained	100%
31	No protecting barrier around facility	Was not feasible at the time of the original review. Current situation allows the installation of a barrier and other safety striping. Parts on order and will be complete 08-19-04.	50%
32	No hazard communication training	Hazard communication training courses completed by personnel; MSDS sheets on site	100%
33	No training or documentation on cleaning up small spills	Spill Prevention, Control, and Countermeasures (SPCC) Plan written	100%
34	No MSD sheets available on site	Safety Data Sheets now available on site	100%

9. TECHNOLOGY TRANSFER

All representatives from the ACTS JIP members except one attended the May 11, 2004 Advisory Board Meeting (ABM).

SPE paper (SPE 90038) that was accepted for presentation in the SPE Annual Technical Conference has been submitted. An abstract was also submitted for the 22nd SPE/IADC Drilling Conference that will be held in Amsterdam.

In addition, we had technical meetings with Hughes-Christensen, ConocoPhillips and Shell. The meetings were productive. Shell is one of the potential future JIP members.

As discussed at the last ABM of ACTS JIP, future research activities will be under the umbrella of TUDRP. Advisory board meetings will continue to be held in November and May of each year.